doi:10.1093/brain/awq139 Brain 2010: 133; 2295–2312 | 2295

BRAIN
A JOURNAL OF NEUROLOGY

S phase entry causes homocysteine-induced death while ataxia telangiectasia and Rad3 related protein functions anti-apoptotically to protect neurons

Weizhen Ye and Stacy W. Blain

Departments of Paediatrics and Cell Biology, State University of New York, Downstate Medical Centre, Brooklyn, NY 11203, USA

Correspondence to: Stacy W. Blain,
Department of Paediatrics and Cell Biology,
State University of New York,
Downstate Medical Centre,
450 Clarkson Avenue,
Box 49, Brooklyn,
NY 11203, USA
E-mail: stacy.blain@downstate.edu

A major phenotype seen in neurodegenerative disorders is the selective loss of neurons due to apoptotic death and evidence suggests that inappropriate re-activation of cell cycle proteins in post-mitotic neurons may be responsible. To investigate whether reactivation of the G1 cell cycle proteins and S phase entry was linked with apoptosis, we examined homocysteine-induced neuronal cell death in a rat cortical neuron tissue culture system. Hyperhomocysteinaemia is a physiological risk factor for a variety of neurodegenerative diseases, including Alzheimer's disease. We found that in response to homocysteine treatment, cyclin D1, and cyclin-dependent kinases 4 and 2 translocated to the nucleus, and p27 levels decreased. Both cyclin-dependent kinases 4 and 2 regained catalytic activity, the G1 gatekeeper retinoblastoma protein was phosphorylated and DNA synthesis was detected, suggesting transit into S phase. Double-labelling immunofluorescence showed a 95% co-localization of anti-bromodeoxyuridine labelling with apoptotic markers, demonstrating that those cells that entered S phase eventually died. Neurons could be protected from homocysteine-induced death by methods that inhibited G1 phase progression, including down-regulation of cyclin D1 expression, inhibition of cyclin-dependent kinases 4 or 2 activity by small molecule inhibitors, or use of the c-Abl kinase inhibitor, Gleevec™, which blocked cyclin D and cyclin-dependent kinase 4 nuclear translocation. However, blocking cell cycle progression post G1, using DNA replication inhibitors, did not prevent apoptosis, suggesting that death was not preventable post the G1-S phase checkpoint. While homocysteine treatment caused DNA damage and activated the DNA damage response, its mechanism of action was distinct from that of more traditional DNA damaging agents, such as camptothecin, as it was p53-independent. Likewise, inhibition of the DNA damage sensors, ataxia-telangiectasia mutant and ataxia telangiectasia and Rad3 related proteins, did not rescue apoptosis and in fact exacerbated death, suggesting that the DNA damage response might normally function neuroprotectively to block S phase-dependent apoptosis induction. As cell cycle events appear to be maintained *in vivo* in affected neurons for weeks to years before apoptosis is observed, activation of the DNA damage response might be able to hold cell cycle-induced death in check.

Received February 16, 2010. Revised April 19, 2010. Accepted April 26, 2010. Advance Access publication July 17, 2010

Keywords: cell cycle; p27; homocysteine; apoptosis; DNA damage response; neurons

Abbreviations: ATM = ataxia-telangiectasia mutant protein; ATR = ataxia telangiectasia and Rad3 related protein; BrdU = 5-bromo-2-deoxyuridine; cdk = cyclin-dependent kinase; Chk = checkpoint protein kinase; Rb = retinoblastoma protein; TUNEL = terminal deoxynucleotidyltransferase-mediated dUTP-biotin nick end labelling

Introduction

Apoptosis or programmed cell death plays a critical role in the development of the mammalian nervous system, but in mature neurons apoptotic mechanisms are held in check. In many neurodegenerative disorders a major phenotype is the selective apoptosis of specific subsets of neuronal populations over years or even decades (Busciglio and Yankner, 1995; Offen *et al.,* 2000; Jimenez del Rio and Velez-Pardo, 2001; Raina *et al.,* 2001; Becker and Bonni, 2004; Jellinger, 2006; Zhu *et al.,* 2006). Alzheimer's disease affects up to 15% of people over the age of 65 and is characterized by the triad of amyloid plaques, neurofibrillary tangles and neuronal cell death. Memory loss and cognitive impairment are caused by neurodegeneration in the hippocampus and cerebral cortex in patients with Alzheimer's disease. The cause of this neurodegeneration is under active debate and molecules implicated in the pathogenesis of Alzheimer's disease include beta-amyloid protein, tau, presenilins, homocysteine, apolipoprotein E and most recently, the proteins that regulate cell cycle progression.

The cell cycle is governed by the action of the cyclin-dependent kinase complexes (cyclin–cdks) (Malumbres and Barbacid, 2009). Cyclins bind to cdks and positively regulate their kinase activity (Sherr and Roberts, 1999). In mammalian cells, cyclin D-cdk4/6 and cyclin E–cdk2 regulate the G1–S phase transition. These kinases phosphorylate substrates, such as the tumour suppressor retinoblastoma protein (Rb), which acts as a brake to S phase entry. In its unphosphorylated state, Rb sequesters transcription factors required for S phase entry, and cells are arrested in G1. Because cyclin–cdks are responsible for all cell cycle transitions, cdk activity is tightly regulated by a combination of mechanisms, including changes in the cyclin level, nuclear to cytoplasmic shuttling, phosphorylation of positive and negative regulatory sites on the cdk partner and interaction with stoichiometric inhibitors (cyclin-dependent kinase inhibitors), such as p27Kip1, p21Cip1, p15Ink4b or p16Ink4a (Sherr and Roberts, 1999). Interaction of cyclin-dependent kinase inhibitors with cdks is the major route by which antiproliferative responses, such as contact, tumour growth factor-β, ultraviolet irradiation or differentiation, affect cdk activity (Besson *et al.,* 2008).

The differentiated neurons in the CNS had been described as post-mitotic cells, believed to have lost their capacity for proliferation. However, loss of cell cycle inhibitors, such as p27 or p19 in knockout animals, caused immature CNS neurons to re-enter the cell cycle, demonstrating that these neurons were being actively maintained by cyclin-dependent kinase inhibitors in a reversible, quiescent state (Zindy *et al.,* 1999; Akashiba *et al.,* 2006*a*, *b*; Ueyama *et al.,* 2007). Increasing evidence suggests a correlation between cell cycle re-entry and the neuronal apoptosis seen in neurodegenerative diseases. Evidence for cell cycle reactivation is found both in Alzheimer's disease mouse models and Alzheimer's disease brains (Copani *et al.,* 1999; Chen *et al.,* 2000; Liu and Greene, 2001; Becker and Bonni, 2004). Altered and inappropriate cyclin D, cdk4 and p27 overexpression and Rb phosphorylation was detected in Alzheimer's disease neurons as compared to age-matched controls (McShea *et al.,* 1997; Nagy *et al.,* 1997, 1998; Raina *et al.,* 2000; Ogawa *et al.,* 2003; Thakur *et al.,* 2008). DNA replication was detected by fluorescent *in situ* hybridization in neurons from Alzheimer's disease model mice (Angelastro *et al.,* 2001; Yang *et al.,* 2003), but was rarely observed in either normal aged brain tissue or in the naturally occurring apoptosis that occurs during development (Herrup and Yang, 2007). Activated DNA replication proteins, such as the mini-chromosome maintenance (MCM2) proteins, have been detected in Alzheimer's disease brains, indicating that inappropriate S phase entry might occur during disease progression (Bonda *et al.,* 2009). In tissue culture models, cell cycle re-entry or cyclin–cdk activation was found associated with the apoptosis seen in PC12 cells and sympathetic neurons in response to deprivation of trophic support (Park *et al.,* 1996), exposure to beta-amyloid protein (Giovanni *et al.,* 1999) or camptothecin treatment (Park *et al.,* 1997). Apoptotic stimulation of cortical neurons caused cyclin D1 to re-locate to the nucleus (Sumrejkanchanakij *et al.,* 2003), and p27 levels were reduced in several neuronal death models including cerebral ischaemia, repolarization and glutamate toxicity (Akashiba *et al.,* 2006*a*, *b*; Qiu *et al.,* 2009). The cell cycle reactivation model suggests that instead of completing the entire cell cycle, the passage into S phase induces apoptosis, contributing to the pathology of diseases such as Alzheimer's disease. However, it is unclear whether cell cycle reactivation is the initiating event that causes neuronal death, or merely a neuroprotective response to apoptosis induction (Raina *et al.,* 2004; Herrup and Yang, 2007).

In this study, we examined the G1 phase of the cell cycle, to determine whether the exit from G0 phase and transit into S phase were responsible for homocysteine-induced neuronal apoptosis in cortical neurons. Homocysteine is a non-essential sulphur-containing amino acid, produced as a natural consequence of methionine metabolism and has been shown to be a strong independent risk factor for dementia and other neurodegenerative diseases (Clarke, 1998; Seshadri *et al.,* 2002; Mizrahi *et al.,* 2004; Agnati *et al.,* 2005). Our results demonstrate that the G1 cell cycle proteins are rapidly activated following homocysteine treatment and neurons could be protected from homocysteine-induced cell death by a variety of methods that inhibit G1 phase progression. We found a 95% co-localization of apoptosis markers with DNA synthesis markers, demonstrating that those cells that entered S phase underwent apoptosis. Interestingly, inhibition of the DNA damage response [ataxia-telangiectasia mutant (ATM) and ataxia telangiectasia and Rad3-related protein (ATR)] did not rescue homocysteine-induced apoptotic death, but instead exacerbated it. Thus, our data suggest that G1 transit and S-phase entry are

critical factors in homocysteine-induced neuronal apoptosis, and the ATM/ATR response may normally function neuroprotectively to prevent or repair inappropriate cell cycle progression.

Materials and methods

Chemicals

Homocysteine, caffeine, camptothecin, olomoucine, 5-bromo-2-deoxyuridine (BrdU), aphidicolin, hydroxyurea, nocodazole and poly-L-lysine were purchased from Sigma (St. Louis, MO). Ku-55933, K2 inhibitor II (Davis *et al.,* 2001) and K4 inhibitor II (Kubo *et al.,* 1999) were purchased from Calbiochem (Gibbstown, NJ). Gleevec™ (STI571 mesylate salt) was a gift from Novartis Pharmaceuticals. Camptothecin, olomoucine, Ku-55933, K2 inhibitor II and K4 Inhibitor II were dissolved in dimethyl sulphoxide. Caffeine was dissolved freshly in medium. Control cultures contained <0.3% dimethyl sulphoxide as a vehicle control, and were not affected within the time range of the experiments described. Homocysteine was prepared at 100 mM in fresh medium. Ku-55933, olomoucine, K2 inhibitor II and K4 inhibitor II were diluted with medium and added into culture 1 h before homocysteine addition.

Antibodies

Monoclonal anti-microtubule associated protein 2, actin and anti-BrdU antibodies were purchased from Sigma (St. Louis, MO). Phospho-checkpoint protein kinase (Chk) 1 (Ser296), phospho-Chk1 (S319), phospho-Rb (Ser795), phospho-p53 (S15), phospho-cdk2 (160), phospho-ATR (S428) and activated caspase-3 (Asp175) antibodies were purchased from Cell Signalling (Danvers, MA). Antibodies to c-Abl (K-12), cyclin D1 (H-295), cdk4 (C-22) and cdk2 (sc-163) were purchased from Santa Cruz Biotechnology (Santa Cruz, CA). Phospho-histone H2A.X (S139) (clone JBW301) antibody was purchased from Millipore (Billerica, MA). Antibodies to cyclin A2 and phospho Chk2 (T68) were purchased from AbCam (Cambridge, MA). p27Kip1 antibodies were purchased from BD transduction laboratories (San Jose, CA). Fluorescent-conjugated Alexa Fluor 488, 568 and 632 anti-mouse and anti-rabbit immunoglobulin G were purchased from Molecular Probes (Carlsbad, CA).

Primary culture of rat cerebral cortical neurons

Time-mated pregnant Sprague Dawley rats were obtained from Charles River Laboratories (Wilmington, MA). Primary neuronal cultures of rat cerebral cortex were prepared as described with some modifications (Carey *et al.,* 2002). In brief, whole brains were isolated from foetal rats at embryonic days 17–18 and the cerebral cortices were treated with 0.25% trypsin (Cellgro, Manassas, VA) and 0.01% deoxyribonuclease I (Sigma) at 37°C for 15 min. Cells were dissected, mechanically dissociated and suspended in Neurobasal medium (Invitrogen, Carlsbad, CA) containing 10% foetal bovine serum. Cortical cells were plated at a density of 1.2×10^7 cells in 100 mm dishes, 4×10^5 cells in 12-well dishes, 10^5 cells in 48-well plates or on glass coverslips precoated with poly-L-lysine. Cultures were maintained at 37°C in humidified 5% CO_2, 95% air. The day after plating, the medium was changed to serum-free Neurobasal medium supplemented with 2% B27 (Invitrogen), 0.5 mM glutamine and 0.002% gentamycin sulphate. Fifty percent of the culture medium was changed every 3 days. Homocysteine or other reagents were added into medium at Days 7–9, as indicated in the text.

Viability measurements

Neuronal survival was determined using the CellTiter-Glo Luminescent Cell Viability Assay from Promega (Madison, WI) per the manufacturer's instructions. Briefly, cells were maintained at room temperature for 10 min, mixed with 40 µl/well CellTiter-Glo reagent for 5 min and incubated for an additional 10 min at room temperature. The luminescence of the lysate was measured with a Glomax luminometer (Promega, Madison, WI). Luminescent intensity was proportional to the number of metabolically viable neurons (Crouch *et al.,* 1993; Andreotti *et al.,* 1995). Each experiment was performed at least three independent times. Neuronal survival after treatment with pharmacological agents was compared to parallel treatment with control medium, and survival was expressed as percent of control ± standard deviation (SD) ($n = 6$ per condition).

Immunoblot and immunoprecipitation analysis

Assays were performed as previously described (James *et al.,* 2008). The preparation of a cytoplasmic and nuclear extraction was done using the CellLytic Nuclear Extraction Kit (Sigma, St. Louis, MO) according to manufacturer's instructions.

Immunofluorescence

Cells cultured on poly-L-lysine-coated glass coverslips or multi-well plates were treated as indicated, fixed with 4% formaldehyde (12 min at room temperature), permeabilized in phosphate buffered saline-0.25% Triton X-100 (5 min at room temperature) and stained with the first antibodies, as specified in the figure legends. They were then visualized by incubation with Alexa Fluor 488, 568, 632 goat anti-mouse IgG or goat anti-rabbit IgG, followed by DNA staining with either ToPro 3 (Molecular Probes), Hoechst 33342-bisbenzimide (Sigma), DapI (Sigma) or propidium iodide (Sigma). For anti-cyclin D1, anti-cdk4 or anti-phospho-Rb staining, cells were stained with the primary antibodies at 4°C overnight, followed by peroxidase-conjugated secondary antibodies (SouthernBiotech, Birmingham, Al). Immunostains were visualized using a fluorescent tyramide reagent (TSA-direct NEL-701, PerkinElmer, Waltham, MA) as described previously (Ye *et al.,* 2009). Confocal images were acquired by a Zeiss 510 laser-scanning microscope.

Comet assay for DNA damage

The CometAssay Kit (Trevigen, Gaithersburg, MD) was used to detect single- and double-stranded DNA breaks in cultured cortical neurons (Tice *et al.,* 2000). Slides were viewed (excitation 425–500 nm) with a Zeiss Axiophot epifluorescence microscope. Two CometSlides were used for each condition. In normal neurons, the fluorescence is confined mostly to the nucleus because undamaged DNA cannot migrate. In neurons with DNA damage, DNA is denatured by the alkali solution used for single-strand break detection, or the neutral solution used for double-strand break detection, and the negatively charged DNA

fragments are released from the nucleus and migrate toward the anode.

Terminal deoxynucleotidyl transferase-mediated dUTP-biotin nick end labelling assay

For dual staining with the terminal deoxynucleotidyltransferase-mediated dUTP-biotin nick end labelling (TUNEL) reagents and BrdU, or dual staining with TUNEL and anti-activated caspase-3 labelling, cells were cultured on glass coverslips, fixed in 4% paraformaldehyde (15 min at room temperature) and permeabilized by incubation with phosphate buffered saline–0.25% Triton X-100 (5 min). Cells were stained with the TUNEL reagents (DeadEnd Fluorometric TUNEL System, Promega) first, as previously described (Ye and Zhang, 2004). For the BrdU staining, after the last wash cells were incubated with 2 M HCl at room temperature for 30 min to denature DNA, washed with phosphate buffered saline, incubated with mouse anti-BrdU (1:75 dilution, diluted in 1% bovine serum albumin/phosphate buffered saline) antibodies (Sigma, St. Louis, MO) for 1 h, washed with phosphate buffered saline and visualized by incubation with Alexa Fluor 593 rabbit anti-mouse IgG (1:2000 diluted in 1% bovine serum albumin/phosphate buffered saline) for 1 h at room temperature. For anti-activated caspase-3 immunoflourescent labelling, cells were incubated with mouse anti-activated caspase-3 antibody, visualized by incubation with Alexa Fluor 593 rabbit anti-mouse IgG and washed with phosphate buffered saline, before slides were mounted with ProLong Gold antifade reagent (Molecular Probes).

Cyclin D1 knockdown

Cyclin D1 antisense oligodeoxynucleotides 5′-GGAGCT GGT GTT CCA TGG-3′ were complementary to the translation start site of the cyclin D1 complementary DNA and sense oligomers 5′-CCA TGG AAC ACC AGCTCC-3′ were used as a control (Shuai *et al.,* 2006). The two sequences were synthesized and optimized by Oligos Etc Inc. (Wolsonville, OR). Antisense oligonucleotide treatment of neurons was performed as previously described (Shan *et al.,* 2003). Cultures were transfected for 48 h. Cyclin D1 expression was determined by immunofluorescence microscopy and immunoblot analysis. Homocysteine (0.25 mM) was added after 48 h. The TUNEL assay was used 3 days later to determine the percentage of apoptotic cells.

Data analysis

P-values were determined by a Student's *t*-test, error bars depict SD.

Results

We determined the effect of homocysteine treatment on cell survival in primary, differentiated cortical neurons. Cortical neurons isolated from embryonic day 18 embryos were placed in culture in Neurobasal medium for 7–10 days. On day 7, more than 90% of the cultured cells were positive for microtubule associated protein 2 staining (Fig. 1C), which is a marker specific for differentiated neurons (Mehra and Hendrickson, 1993; Martinez *et al.,* 1997). Seven-day-old cultures were then treated with homocysteine at different doses and for the indicated times. The addition of homocysteine significantly reduced neuronal survival, in a dose- and time-dependent manner (Fig. 1A and B). Approximately 30% of the neurons died within 48 h in 0.25 mM homocysteine, and 80% died after 5 days of treatment. The 0.25 mM concentration of homocysteine was in the previously published range (Kruman *et al.,* 2000). As cell cycle activity is often density-dependent, we examined the response to homocysteine at different densities of cultured neurons, and reduced survival was seen in all conditions (Fig. 1A). Apoptosis activity in the homocysteine-treated neurons was detected by immunolabelling and confocal microscopy using anti-cleaved caspase-3 antibodies, suggesting that the neuronal death caused by homocysteine treatment was due to apoptotic activation (Fig. 1C and D). Less than 4% of the untreated cells were positive for anti-cleaved caspase-3 labelling and this low level presumably results from the low level of spontaneous death seen in our culture conditions. Homocysteine treatment increased cleaved caspase-3 detection to ~15% (Fig. 1C and D), which corresponded with the neuronal cell death seen in these populations (Fig. 1A and B).

To determine whether homocysteine induces cell cycle re-activation in differentiated cortical neurons, we used BrdU to label newly synthesized DNA during the S phase of the cell cycle (Gonchoroff *et al.,* 1986). Few untreated neurons labelled with anti-BrdU antibodies, suggesting that the majority of the differentiated cortical neurons had exited the cell cycle and were not proliferating (Fig. 1C and D). A significant increase (>12%) of BrdU positive nuclei was found in the homocysteine-treated neurons (Fig. 1C and D), suggesting that these cells were actively synthesizing DNA. While in theory, DNA synthesis in response to DNA damage might increase the BrdU signal in the homocysteine treated cells, previous studies have shown that DNA repair does not result in significant BrdU labelling (Cooper-Kuhn and Kuhn, 2002), suggesting that we were detecting DNA replication. Rb regulates cell cycle progression through the G1–S phase checkpoint (Sherr and Roberts, 1995, 1999), and phosphorylation of Rb by cdks causes Rb inactivation and subsequent cell cycle progression (Knudsen and Wang, 1997). We used anti-phospho-Rb (S795) immunolabelling to measure Rb phosphorylation in the presence or absence (control) of homocysteine treatment (Fig. 1C and D). Homocysteine treatment significantly increased the proportion of anti-phospho Rb (S795) positive nuclei from 18% in untreated cells to >40% in treated cells (Fig. 1C and D), suggesting that homocysteine treatment caused cell cycle reactivation and entry into S phase.

To correlate homocysteine-induced apoptosis with cell cycle phase, we stained cells with multiple antibodies simultaneously followed by confocal microscopy immunofluorescence. Co-localization of activated caspase-3 staining with BrdU labelling was seen in the nuclei of homocysteine-treated neurons (Fig. 2A). Cells were stained with anti-BrdU (blue), anti-phospho Rb (S795) (red) and TUNEL (green), and colocalization analysis of this triple labelling was performed in the homocysteine-treated neurons (Fig. 2B). The results show that colocalization between BrdU positive and TUNEL positive nuclei was almost 95% (Fig. 2B, right panel and 2C), suggesting that cells that initiated DNA synthesis and entered S phase were also undergoing apoptosis. Within the same group, less than 20% of cells contained both TUNEL and

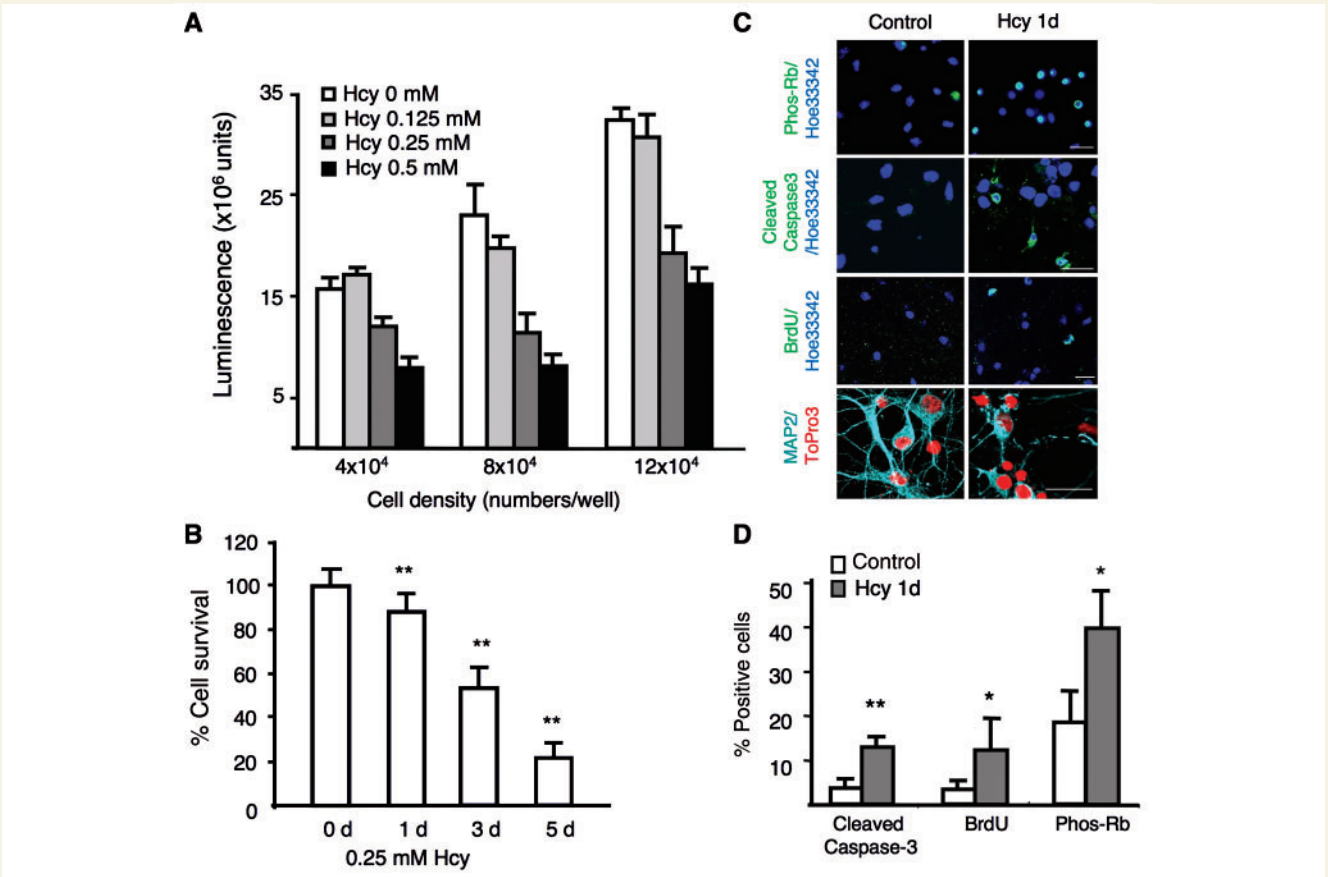

Figure 1 Homocysteine induced apoptotic death in primary cortical neurons. (**A**) Cultured neurons, plated at the indicated densities were exposed to the indicated concentrations of homocysteine (Hcy) for 38 h, before they were assessed for cell viability using the CellTiter-Glo assay. (**B**) Cultured neurons, plated at 8×10^4 cells/wells in 48-well plates, were exposed to 0.25 mM homocysteine for 1, 3 or 5 days before they were assessed for cell viability. (**C**) Cultured neurons were exposed for 20 h to 0.25 mM homocysteine or saline (control), then stained using anti-phospho Rb (S795) (top panel, green), anti-cleaved Caspase 3 (second panel, green), anti-BrdU (third panel, green) antibodies or anti-microtubule associated protein2 antibodies (bottom panel, blue). Hoescht33342 (blue) (panels 1–3) and ToPro3 (red) (bottom panel) stained nuclei. (**D**) The positive labelling ratio of anti-cleaved Caspase-3, anti-BrdU and anti-phospho-Rb (S795) staining cells seen in homocysteine-treated neurons. Scale bar = 20 μm. Data are the result of three different cell culture experiments. $*P < 0.01$, $**P < 0.001$, *Y* error bar = SD. Student's *t*-test used.

phospho-Rb (S795) staining. Likewise, <20% of the homocysteine-treated cells colocalized the BrdU and phospho-Rb (S795) markers (Fig. 2B, left, middle panels and 2C). While ~40% of the homocysteine-treated cells became Rb positive (Fig. 1C and D), the colocalization studies (Fig. 2B and C) suggest that Rb phosphorylation at the S795 site itself was not sufficient to induce apoptosis; and entry into S phase, as measured by BrdU incorporation and DNA synthesis, was required to cause neuronal cell death in differentiated cortical neurons. Homocysteine induced cell cycle re-entry in ~40% of the treated cells, but a smaller percentage (15–20%) entered S phase. This S phase entry, however, seemed sufficient to initiate apoptosis.

To analyse cell cycle re-entry in the presence of homocysteine further, we examined many of the major cell cycle players that regulate the G1–S phase transition: cyclin D–cdk4, cyclin A–cdk2 and p27Kip1 (Sherr and Roberts, 1999). Differentiated neurons were treated with homocysteine and analysed at different time points post treatment (Figs 3 and 4) to determine the expression levels, subcellular locations, interaction status and kinase activity of cdks and cyclin-dependent kinase inhibitors by immunoprecipitation, immunoblot and confocal microscopy. For microscopic analysis, co-staining with 4′,6-diamidino-2-phenylindole or ToPro3 was used to define nuclei (Fig. 3). We found that cyclin D1 immunoreactivity was detected mainly in the cytoplasm in differentiated cortical neurons (Fig. 3A and C). In homocysteine-treated neurons, increased nuclear and decreased cytoplasmic cyclin D1 was detected by 2 h, which continued to increase up to 20 h, suggesting that homocysteine treatment caused a cytoplasmic to nuclear translocation, similar to the mitogen-induced cytoplasmic to nuclear translocation of cyclin D1 observed in non-neuronal lineages (Gladden and Diehl, 2005). Similar homocysteine-dependent translocations were seen with cdk4 and cdk2 (Fig. 3A). Cdk4 was localized in the cytoplasm of untreated neurons (0 h), but quickly accumulated in the nucleus in the presence of

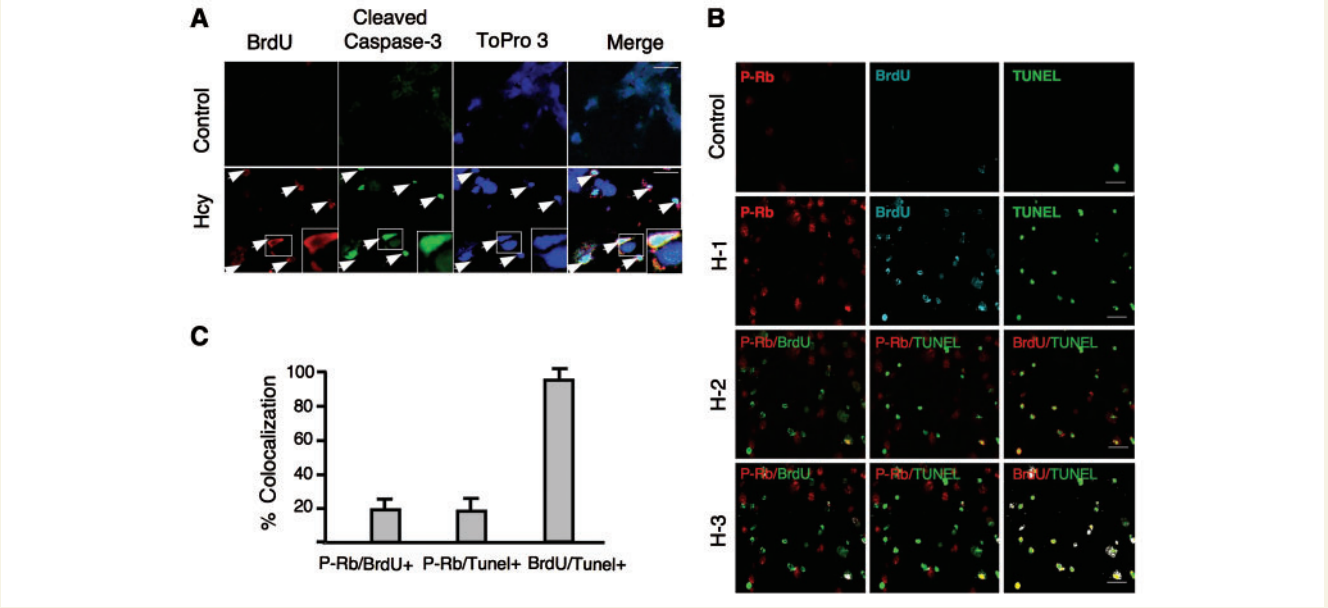

Figure 2 Multi-staining with BrdU, apoptosis and cell cycle markers in homocysteine-treated cortical neurons. Neurons were exposed for 24 h to saline (control) or 0.25 mM homocysteine (Hcy). BrdU was added to the medium to label DNA synthesis. (**A**) Double staining with anti-BrdU (red) and anti-activated caspase-3 (green) antibodies. DNA was stained with ToPro-3 (blue). Co-localization of BrdU with activated caspase-3 immunofluorescence was found in homocysteine-treated neurons (arrowhead). (**B**) Immunofluorescence triple staining with anti-phospho Rb (red), anti-BrdU (blue) antibodies and TUNEL (green) assay. Control is saline neurons. H-1 is the visualization of each marker individually. H-2 is the visualization of two parameters under fluorescence [left: BrdU (green) and phospho-Rb (P-Rb, red); middle: phospho-Rb (red) and TUNEL (green); left: BrdU (red) and TUNEL (green)]. H-3 images are the results of the co-localization analysis of H-2 images by Image-J software. (**C**) Quantitative analysis of percent positive co-localization based on results of Image-J. Scale bar = 20 μm. At least 300 cells were counted from three different images to generate the average. Standard deviation included.

homocysteine (2 h), and was predominantly nuclear by 20 h of treatment (Fig. 3A). Cyclin A localization was nuclear in the untreated neurons, and was unaltered by homocysteine treatment. Cdk2 was predominantly cytoplasmic in untreated cells (0 h), but by 2 h of homocysteine treatment it was detected in the nucleus. Thus, in response to homocysteine treatment, cyclin D, cdk4 and cdk2 appeared to translocate to the nucleus, where they could potentially partner to form cyclin D–cdk4 and cyclin A–cdk2 complexes and phosphorylate their nuclear targets (Sherr and McCormick, 2002). Rb phosphorylation itself was detected within 2 h of homocysteine treatment, suggesting that these neurons had re-entered the cell cycle and reached the G1–S phase border (Fig. 3A).

p27Kip1 interacts with both cdk4 and cdk2-associated complexes, and is a potent inhibitor of these kinases in growth-arrested cells (Blain, 2008; James *et al.,* 2008). It has been suggested that its high expression in differentiated cells may help to maintain cdk4 and cdk2 in their catalytically inactive forms, holding neuronal cells in the G0 quiescent state (Zindy *et al.,* 1999). To determine the localization and expression of p27, we stained homocysteine-treated neurons with anti-p27 antibodies. p27 was detected predominately in the nucleus of untreated differentiated neurons, with weaker but detectable cytoplasmic expression observed (Fig. 3A and B). In the presence of homocysteine by 20 h total p27 staining was reduced significantly (Fig. 3A). In apoptotic cells, the down-regulation of p27 appeared to occur significantly in the nucleus (Fig. 3B). As epithelial cells and lymphocytes exit G0 phase, p27 levels decrease to lower but detectable levels, restoring catalytic activity to inactive cdk complexes (Nickeleit *et al.,* 2007; Besson *et al.,* 2008), and these data in differentiated neurons were consistent with the idea that these cells had re-entered the cell cycle in response to homocysteine treatment.

Homocysteine-treated cells were analysed by immunofluorescence with multiple antibodies to determine co-localization of the different G1 cell cycle proteins (Fig. 3C). Double-staining with cyclin D1 and p27 antibodies demonstrated that cyclin D1 and p27 resided in different compartments in untreated cells: cyclin D1 was predominantly in the cytoplasm, while p27Kip1 was predominately in the nucleus (Fig. 3C). After homocysteine treatment, however, both cyclin D1 and p27 could be detected in the nuclear compartment in cells with intact nuclei as detected by ToPro nuclear staining (Fig. 3C). This nuclear to cytoplasmic translocation appeared to be a phenomenon specific for cyclin D1 and not cyclin D2 (Fig. 3D). Cyclin D2 was predominantly nuclear in untreated cells, and homocysteine treatment did not alter its localization (Fig. 3D).

While p27 levels appeared to remain high and nuclear in homocysteine-treated neurons that were not undergoing apoptosis, as measured by chromatin condensation (Fig. 3C), we predicted that p27 levels might decrease specifically in those neurons that were initiating apoptosis. Using anti-p27 antibodies, we found

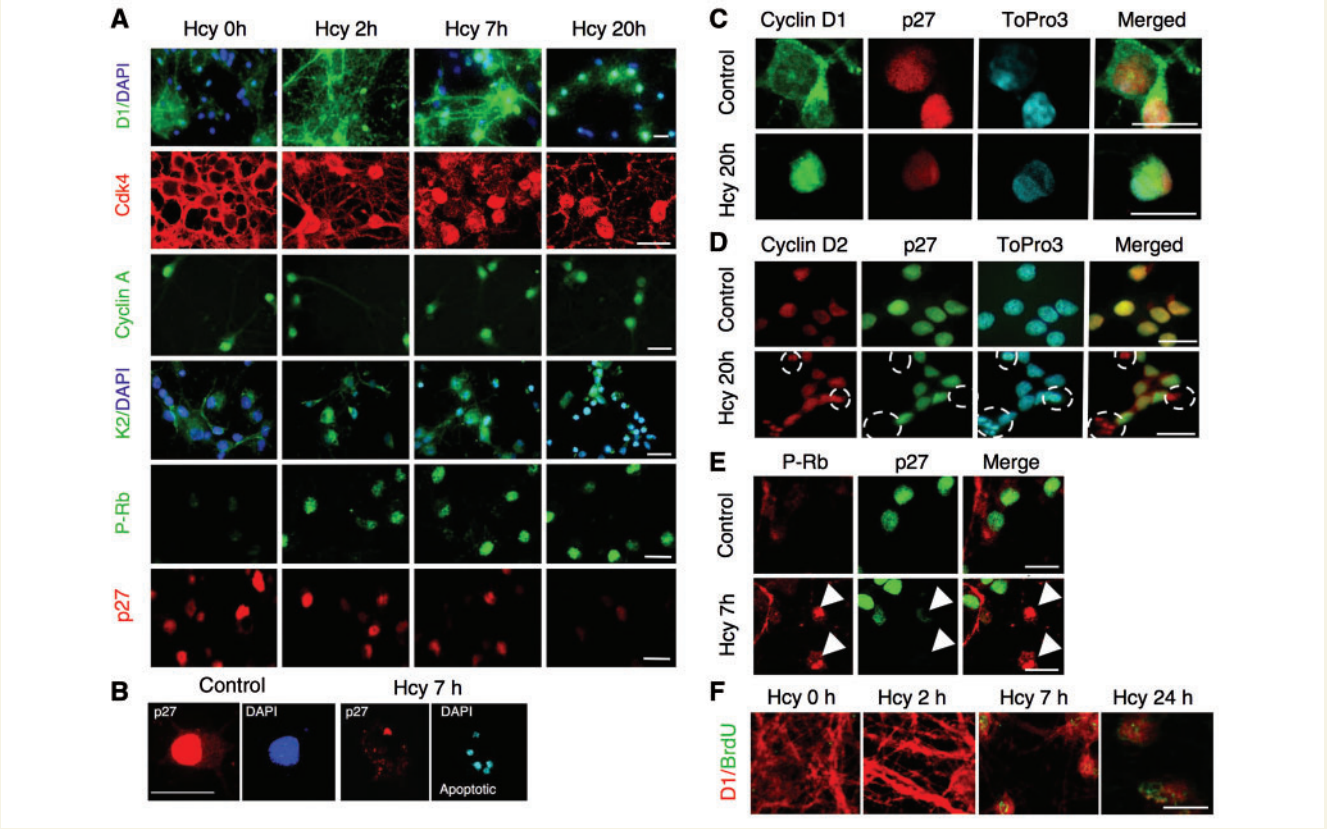

Figure 3 Immunoreactivity of G1 cell cycle proteins in cultured neurons. (**A**) Cultures were exposed for the indicated time courses to 0.25 mM homocysteine (Hcy) before labelling with antibodies to cyclin D1, cdk4, cyclin A, cdk2, phospho-Rb (P-Rb) and p27Kip1. Nuclei were labelled with 4′,6-diamidino-2-phenylindole (DAPI) or ToPro3. (**B**) Labelling with p27Kip1 antibodies. (**C**) Co-localization with p27 (red), cyclin D1 (green) and ToPro3 (blue). (**D**) Co-localization with p27Kip1 (green), cyclin D2 (red) and ToPro3 (blue). White dashed circles indicate apoptotic nuclei, as measured by condensation of the chromatin visible by nuclear staining. (**E**) Co-localization with p27 (green) and phospho-Rb (red). Arrowheads indicate nuclei with reduced p27 levels and increased phospho-Rb. (**F**) Co-localization with cyclin D1 (red) and BrdU (green) antibodies at different time points post homocysteine treatment. Scale bar = 20 μm.

two types of p27 staining cells: homocysteine-treated cells that appeared to retain nuclear p27 (Fig. 3D, green) or alternatively those that had significantly reduced p27 expression (Fig. 3D, white dashed circles). Lack of nuclear p27 expression appeared to correlate with apoptosis, as measured visually by chromatin condensation seen in the ToPro stained cells (Fig. 3D, white dashed circles, merge). Homocysteine-treated cells with detectable p27 staining had intact nuclei, while cells with reduced or absent p27 staining were undergoing apoptosis. This suggested that p27 loss might be a prerequisite for apoptosis in differentiated neurons.

When homocysteine-treated and untreated neurons were stained with both anti-p27 and anti-phospho-Rb antibodies, an inverse correlation was observed (Fig. 3E). Little phospho-Rb was detected in untreated cells. By 7h post treatment phospho-Rb staining was seen, but only in cells that had severely reduced p27 expression (Fig. 3E, green arrows). In cells that retained high nuclear p27 expression, Rb phosphorylation was not detected, suggesting that reduction of p27 expression correlated with the appearance of phospho-Rb as a marker of the G1–S phase transition.

To demonstrate directly that neurons with activated G1 cell cycle programs were entering S phase, treated and untreated cells were co-stained with anti-cyclin D1 and BrdU antibodies (Fig. 3F). Little BrdU staining and predominantly cytoplasmic cyclin D1 were detected in untreated cells (0 h). Homocysteine treatment, however, caused the mobilization of cyclin D1. By 7 h of treatment, cyclin D1 was predominantly nuclear and BrdU specifically co-localized in these cells. Together these data suggest that homocysteine treatment caused the translocalization of cyclin D1, cdk4 and cdk2 to the nucleus, where they could potentially interact with their nuclear targets. Concomitant with this, a reduction to lower p27 levels was seen and Rb became phosphorylated. These data suggest that the differentiated neurons had exited the G0 phase, passing through G1 phase on their way to S phase. Co-localization of these events occurred in cells that underwent apoptosis, suggesting that the reactivation of the G1 cell cycle players and their activity was required for homocysteine-induced apoptosis.

Cyclin–cdks primarily phosphorylate nuclear targets during cell cycle progression. To examine the localization of the G1 cyclin–cdk complexes further, homocysteine-treated and untreated neurons were harvested at different times post homocysteine addition, and nuclear and cytoplasmic extracts were analysed by immunoblot analysis with antibodies to cyclin A, cyclin D1, cdk4 and cdk2

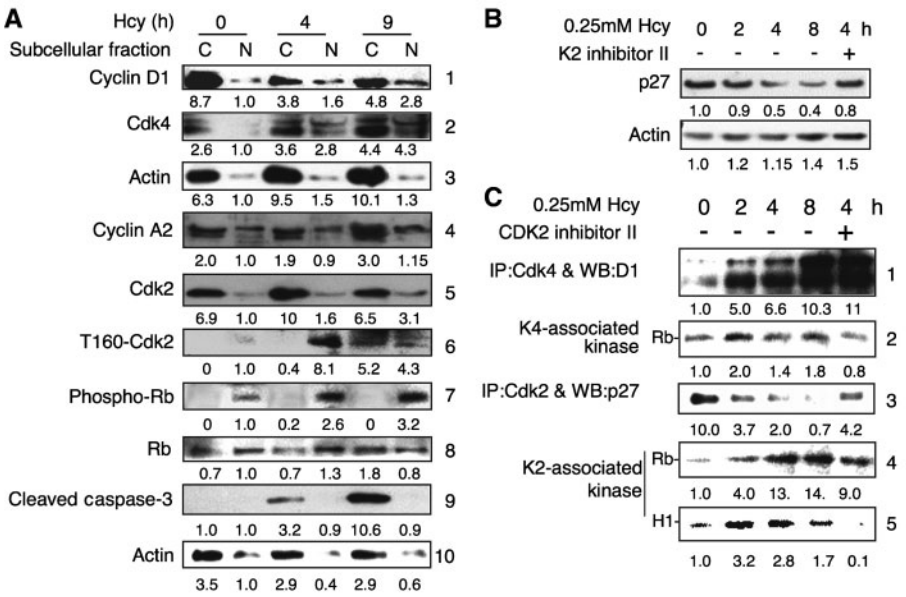

Figure 4 Expression and activities of cell cycle proteins in homocysteine-treated cortical neurons. Differentiated cortical neurons were pretreated with 4 μM cdk2 inhibitor II 1 h before adding homocysteine (Hcy) for the indicated times. (**A**) Immunoblot analysis of nuclear (N) and cytoplasmic (C) fractions of homocysteine-treated neurons, with antibodies against cyclin D1 (lane 1), cdk4 (lane 2), cyclin A2 (lane 4), cdk2 (lane 5), phospho-cdk2 (lane 6), Rb (lane 8), phospho-Rb (lane 7) and cleaved caspase 3 (lane 9). Actin served as a loading control. (**B**) Immunoblot analysis of p27Kip1 protein in homocysteine treated cells. Neurons were treated with K2 inhibitor II before homocysteine addition. (**C**) Lysates from treated cells were immunoprecipitated (IP) with cdk4 (lanes 1 and 2) or cdk2 (lanes 3–5) antibodies, and analysed by immunoblot analysis (WB) with cyclin D1 (lane 1) or p27 (lane 3) antibodies, or used in *in vitro* kinase assays (lanes 2, 4 and 5). Densitometric quantitation of the immunoblots was performed using Image J software.

(Fig. 4A). Cyclin D1 was localized predominantly in cytoplasmic extracts in untreated neurons. Homocysteine treatment decreased its total levels, while significantly increasing its detection in the nucleus (Fig. 4A, lane 1). Cdk4 and cdk2 were also detected primarily in cytoplasmic extracts in untreated neurons, but by 4 and 9 h of treatment increased nuclear detection was observed (Fig. 4A, lanes 2 and 5). Cyclin A was detected in nuclear extracts in untreated neurons and the addition of homocysteine did not alter its distribution (Fig. 4A, lane 4), consistent with results seen by immunofluorescence microscopy. Cdk2 must be phosphorylated on a conserved threonine residue (T160) in order to be catalytically active (Sethi *et al.,* 2005). Using antibodies specific for cdk2 T160 phosphorylation, we did not detect active cdk2 in untreated cells, but it was detected in homocysteine-induced nuclear extracts within 4h of treatment, indicating that cdk2 had regained activity (Fig. 4A, lane 6), consistent with late G1 phase. Phosphorylated cdk2 was also detected in cytoplasmic extracts at 9 h of treatment, consistent with the increased activation and potential nuclear to cytoplasmic shuttling of this complex (Fig. 4A, lane 6). While the total level of Rb protein was unchanged by homocysteine treatment, nuclear (Fig. 4A, lane 8) phosphorylated Rb detection increased by 4 h of treatment (Fig. 4A, lane 7). These data were consistent with the results seen by confocal microscopy: the cyclins and cdks appeared to increase their nuclear expression and activation in the presence of homocysteine. We did not detect any cleaved caspase-3 expression in nuclear or cytoplasmic extracts in untreated neurons, but significant caspase-3 was detected in cytoplasmic extracts by 4 h of homocysteine treatment (Fig. 4A, lane 9), consistent with homocysteine's ability to induce apoptosis following cell cycle re-entry.

Immunoprecipitation of treated and untreated lysates with cdk4 antibodies, followed by cyclin D1 immunoblot analysis, demonstrated that cyclin D1–cdk4 complex formation increased in the presence of homocysteine (Fig. 4C, lane 1). As the cdk4 monomer has minimal activity, increased complex formation should correspond to increased kinase activity (Bockstaele *et al.,* 2006). Immunoprecipitation with cdk4 antibodies, followed by the addition of recombinant Rb substrate and γ-ATP in an *in vitro* kinase assay, demonstrated that homocysteine treatment increased cdk4 catalytic activity as well (Fig. 4C, lane 2).

Immunoblot analysis with antibodies specific for phosphorylated T160 cdk2 suggested that homocysteine-treatment increased cdk2 catalytic activity as well (Fig. 4A, lane 6). To demonstrate this directly, immunoprecipitation with cdk2 antibodies, followed by the addition of either recombinant Rb or Histone H1 substrates and γ-ATP in *in vitro* kinase assays, demonstrated that cdk2 became catalytically active following homocysteine-treatment (Fig. 4C, lanes 4 and 5). Immunoblot analysis of total p27 levels demonstrated that p27 expression, which was high in untreated cells, decreased following homocysteine treatment (Fig. 4B), and this loss of p27 corresponded to a concomitant reduction of p27 in cdk2-associated complexes, as detected by cdk2 immunoprecipitation (Fig. 4C, lane 3). In untreated neurons, significant p27 was associated with cdk2, but this decreased to undetectable levels by 8 h of homocysteine treatment (Fig. 4C, lane 3). As p27 is a constitutive cdk2 inhibitor (Besson *et al.,* 2008), the lack of p27 in the

cdk2 complex permits reactivation of catalytic activity, causing Rb phosphorylation and S phase progression. Our data suggest that homocysteine treatment rapidly reactivates cdk4 and cdk2 activity, permitting G1–S phase transitioning and Rb phosphorylation.

We postulated that if G1 cdk activation was required for apoptosis, inhibition of cdk activity might prevent homocysteine-induced neuronal death. We pre-treated neurons with several small molecule cdk inhibitors before the addition of homocysteine (Fig. 5A). Olomoucine is an inhibitor of cdks 1/2/5 and extracellular-signal-regulated kinase 1/microtubule associated protein kinase (Vesely *et al.,* 1994). It is a poor inhibitor of other protein kinases, and has been shown to prevent death due to nerve growth factor deprivation of differentiated PC12 cells and sympathetic neurons (Park *et al.,* 1996). K2 inhibitor II (Davis, *et al.,* 2001) and K4 inhibitor II (Kubo *et al.,* 1999) selectively inhibit cdk2 and cdk4, respectively. Pretreatment with olomoucine, K2 inhibitor II or K4 inhibitor II all protected neurons from homocysteine-induced death (Fig. 5A). Only 70% of cells remained viable after 48 h in the presence of 0.25 mM homocysteine. Treatment of cells with cdk inhibitors, however, increased cell survival (96.3% + K2 inhibitor II, $P < 0.002$; 93% + K4 inhibitor II, $P = 0.01$; or 92% + olomoucine, $P < 0.005$) (Fig. 5A, left), suggesting that cdk activity was required for homocysteine-dependent apoptosis. K2 inhibitor II also rendered cells resistant to the neuronal death induced at higher concentrations of homocysteine (96.5% cells survival + K2 inhibitor II compared with 56.2% cells survival in 1 mM homocysteine alone) (Fig. 5A, right).

Immunoprecipitation with cdk4 antibodies, followed by cyclin D1 immunoblot analysis demonstrated that the homocysteine-dependent increase in cyclin D–cdk4 complex formation persisted in the presence of K2 Inhibitor II, when cdk2 was inhibited (Fig. 4C, lane 1), although catalytic activity of this complex was reduced (Fig. 4C, lane 2). Co-treatment with homocysteine and the K2 inhibitor II, however, prevented the homocysteine-dependent decrease in p27 levels (Fig. 4B), and immunoprecipitation of lysates with cdk2 antibodies, followed by p27 immunoblot analysis, demonstrated that p27 remained associated with cdk2 complexes (Fig. 4C, lane 3). p27 itself is a substrate of cdk2, and its phosphorylation by cdk2 increases its proteasomal degradation (Frescas and Pagano, 2008). Immunoprecipitation with cdk2 antibodies, followed by the addition of either recombinant Rb or histone H1 substrates and γ-ATP in *in vitro* kinase assays, confirmed the loss of cdk2 catalytic activity following homocysteine and K2 inhibitor II treatment. Thus, inhibition of cdk2 or cdk4 activity blocked cell cycle progression and correlated with increased cell survival in the presence of homocysteine treatment.

As an alternative to inhibit the G1 cdks, we attempted to reduce cyclin D1 expression by using antisense oligonucleotides (Fig. 5B). Sense and antisense oligonucleotides against cyclin D1 were transfected into differentiated neurons. Two days later cells were stained with anti-cyclin D1 antibodies and analysed by confocal immunofluorescence or harvested for immunoblot analysis with cyclin D1 antibodies (Fig. 5B, left). A significant reduction in cyclin D1 expression was detected by both methods and quantitated (Fig. 5B, left). After treatment with 0.25 mM homocysteine for 3 days, differentiated neurons transfected with antisense oligonucleotides showed significantly less apoptosis than cells that had been transfected with sense oligonucleotides (Fig. 5B, right). This was consistent with the idea that cyclin D1–cdk4 played an essential role in causing cell cycle re-entry and the concomitant neuronal apoptosis.

Other groups have suggested that the tyrosine kinase c-Abl becomes activated during the neuronal cell death induced by stressors such as β-amyloid fibrils (Alvarez *et al.,* 2004; Cancino *et al.,* 2008). To determine if Abl was involved in the regulation of homocysteine-dependent neuronal apoptosis, we examined untreated and homocysteine-treated cells by immunoblot analysis using Abl antibodies, and found that the expression of c-Abl increased with treatment time (Fig. 5C). We next treated neurons with Gleevec™ (STI571 mesylate salt), an inhibitor of c-Abl kinase activity (Avramis *et al.,* 2003; Hagerkvist *et al.,* 2007) before homocysteine treatment and measured cell survival. Treatment with Gleevec™ rescued neurons from homocysteine-induced cell death in a dose-dependent manner (Fig. 5D). Using immunofluorescent staining with multiple antibodies, we further evaluated the effects of Gleevec™ on G1 cell cycle activation (Fig. 5E). Gleevec™ treatment blocked the translocation of cyclin D1 and cdk4 from the cytoplasm to the nucleus in homocysteine-treated neurons (Fig. 5E), suggesting that c-Abl inhibition affected G1 phase progression. Gleevec™ treatment also reduced the detection of phospho-Rb after 7 h of homocysteine treatment (Fig. 5F), suggesting that these neurons had not progressed to nor activated the G1–S phase checkpoint. Thus, by chemical cdk inhibition of cdk2 and cdk4, decreasing cyclin D1 expression, or preventing cyclin D–cdk4 nuclear translocation via inhibition of c-Abl, we were able to block neuronal cell death, directly linking G1 cdk activation to homocysteine-induced apoptosis.

We wanted to determine whether blocking S phase progression was also sufficient to block homocysteine-induced death. We pre-treated neurons with DNA replication inhibitors, such as aphidicolin, 1 mM hydroxyurea or 1 μM nocodazole, and 2 h later 0.25 mM homocysteine was added to the cultures as indicated (Fig. 6). Aphidicolin specifically inhibits DNA polymerase-α (Oguro *et al.,* 1979; Kowalzick *et al.,* 1982), hydroxyurea blocks ribonucleotide reductase (Adams and Lindsay, 1967) and nocodazole inhibits microtubule dynamics and arrests the cell cycle at G2/M phase. Unlike the G1 phase inhibitors, none of these DNA replication inhibitors prevented neuronal death induced by homocysteine treatment (Fig. 6). In fact, treatment of neurons with nocodazole was toxic and co-treatment with homocysteine increased cell death even further. This suggests that once a cell entered S phase and began to replicate DNA, apoptosis was not preventable.

The DNA damage response pathway is activated by both physical DNA damage (DNA lesions and/or double- or single-stranded DNA breaks) or in response to DNA replication stress, due to stalled replication forks. The DNA damage response has been shown to be essential for the neuronal apoptosis due to DNA damaging agents, such as camptothecin (Rich *et al.,* 2000; Roos and Kaina, 2006). We wanted to determine whether homocysteine treatment also caused DNA damage in cortical neurons. Using the Comet assay (Angelis *et al.,* 1999; Lemay and Wood, 1999), which detects DNA single-strand breaks and incomplete excision repair sites, we showed that damage was detectable

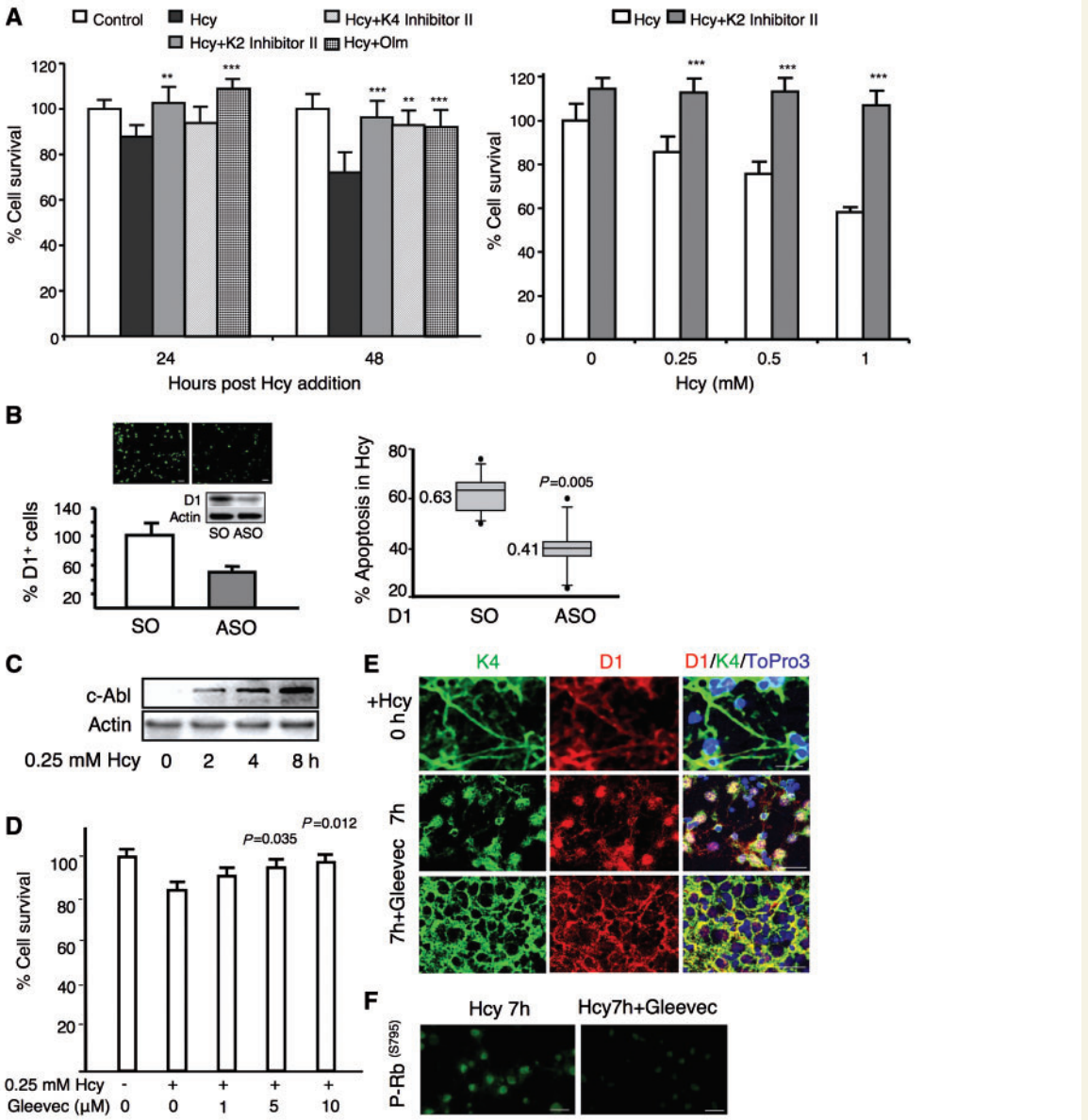

Figure 5 G1 cell cycle inhibitors protect neurons from homocysteine-induced neuronal death. (**A**) Left: neurons were pretreated for 1 h with saline (control), 4 μM K2 inhibitor II, 200 nM K4 inhibitor II or 1 μM olomoucine before 0.25 mM homocysteine (Hcy) was added for 24 or 48 h, and then cell viability was assessed using the CellTiter-Glo assay. Right: cultures were pretreated with saline (control) or 4 μM K2 inhibitor II for 1 h, before increasing amounts of homocysteine were added for 24 h, and then cell viability was assessed. $^{**}P<0.01$, $^{***}P<0.001$, *Y* error bar = SD. Student's *t*-test used. Each data mean of six-wells. Similar results were obtained from three independent experiments. (**B**) Left: neurons were transfected with sense oligomers (SO) l or with cyclin D1 antisense oligomers (ASO) for 48 h. Immunofluorescence and immunoblot analysis with cyclin D1 antibodies confirmed the reduction in cyclin D1 expression and is quantitated. Right: cells transfected with cyclin D1 antisense oligomers had reduced homocysteine-induced apoptosis. Homocysteine (0.25 mM) was added after 48 h. The percentage of apoptotic cells was determined by double labelling with TUNEL and nuclear staining. Data were obtained from three different experiments; *P*-value is from Student's *t*-test. (**C**) Immunoblot analysis with c-Abl antibodies. (**D**) Neurons were pretreated with 10 μM Gleevec™ before homocysteine addition. Cell survival was assessed after 1 day using the CellTiter-Glo assay. *P*-values were determined by Student's *t*-test, ± SD. (**E**) Immunofluorescent microscopy of homocysteine and Gleevec™ treated cells using blocked cyclin D1 (red) and cdk4 (green) antibodies. ToPro3 labelled the nuclei. (**F**) Immunolabelling with phospho-Rb (Ser795) antibodies. Scale bar = 20 μm.

within 4 h of homocysteine treatment (Fig. 7A). More than 70% of the homocysteine-treated cells stained positively in this assay, whereas only a few Comet positive cells (<8%) were detected in non-treated neurons (Fig. 7A). Phosphorylation of H2AX (γ-H2AX) is an early sign of DNA damage induced by stalling replication forks (Bartek and Lukas, 2007; Tanaka *et al.*, 2007; Chanoux *et al.*, 2009). By immunoblot analysis with γ-H2AX antibodies, we detected an increase in γ-H2AX following

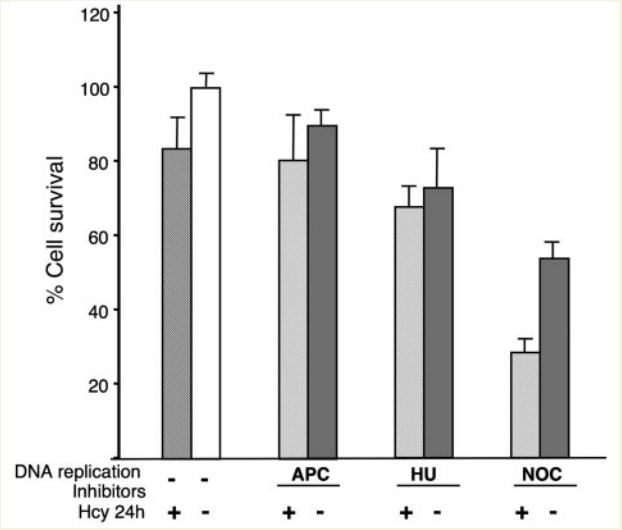

Figure 6 DNA replication inhibitors do not rescue neurons from homocysteine-induced neuronal death. Replicate cultures were treated with and without 0.25 mM homocysteine (Hcy) in the presence and absence of 10 μM aphidicolin (APC), 1 mM hydroxyurea (HU) or 1 μM nocodazole (NOC). Each data point is the mean ± SD ($n = 6$). Cell viability was assessed using CellTiter-Glo assay. Similar results were obtained from three independent experiments.

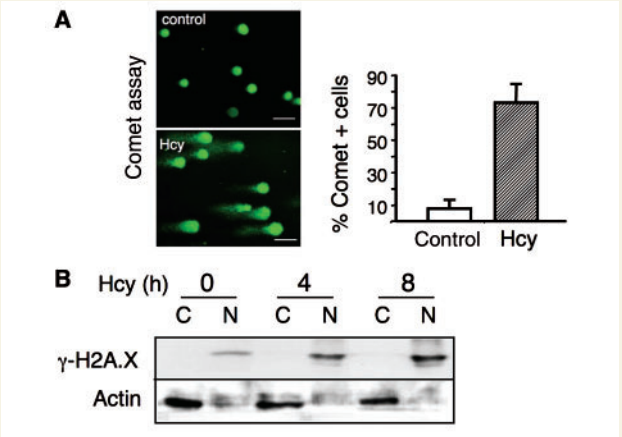

Figure 7 Homocysteine causes DNA damage in cortical neurons. (**A**) Alkaline Comet assay in absence or after 1 h of 0.25 mM homocysteine. DNA is stained with SYBR green. Scale bar = 20 μm. Total green cells were counted and the percentage of Comet positive cells was determined and plotted. Data are mean ± SD ($n = 6$). (**B**) Immunoblot analysis of nuclear and cytoplasmic fractions of treated neurons with γ-H2AX antibodies.

homocysteine treatment (Fig. 7B) suggesting that homocysteine-dependent DNA damage may be due to inappropriate DNA synthesis.

The central proteins of the DNA damage response are ATM and ATR (Rotman and Shiloh, 1999; Pandita, 2002; Brown and Baltimore, 2003). While ATM and ATR share most downstream effectors, the ATM-Chk2 pathway is primarily activated by DNA double-strand breaks and the ATR-Chk1 pathway responds to stalled DNA replication forks (Shiloh, 2003; Bartek and Lukas, 2007). To determine the role of the DNA damage response pathway in homocysteine-induced apoptosis, we treated neurons with homocysteine and Ku-55933, an inhibitor of ATM protein (Hickson *et al.,* 2004) (Fig. 8A). We expected that if activation of the DNA damage response was responsible for triggering the cell death program, inhibition of ATM activity would block homocysteine-induced apoptosis. We found that Ku-55933 treatment did not rescue homocysteine-induced apoptosis, and in fact exacerbated it in a dose-dependent manner (Fig. 8A and B). Ku-55933 treatment in the absence of homocysteine had no affect on cell survival (Fig. 8A). Similar results were seen with caffeine treatment, which is a powerful inhibitor of ATR kinase (Sarkaria *et al.,* 1999; Lu *et al.,* 2008) (Fig. 8C).

By immunoblot analysis with anti-cleaved caspase-3 antibodies using lysates from treated and untreated neurons, we saw that homocysteine-induced caspase-3 activation 8 h post treatment (Fig. 8E). Co-treatment with homocysteine and K2 inhibitor II prevented the detection of activated caspase-3, consistent with the reduced apoptosis seen in the presence of this inhibitor (Fig. 5A). Co-treatment with homocysteine and Ku-55933 or homocysteine and caffeine increased caspase-3 activation (Fig. 8E), consistent with the exacerbation of homocysteine-dependent apoptosis caused by inhibition of the ATM/ATR pathway seen in these cells (Fig. 8A–C).

Thus, inhibitors of ATR/ATM did not rescue homocysteine-induced neuronal cell death, suggesting that the DNA damage response pathway was not inducing apoptosis and might, in fact, normally function to prevent or slow homocysteine-induced apoptosis. This was in contrast to what was seen in camptothecin treated neurons (Fig. 8D). Camptothecin is a topoisomerase I inhibitor that induces apoptosis of cultured cortical neurons in a DNA damage dependent manner (Morris and Geller, 1996; Staker *et al.,* 2002; Zhang *et al.,* 2006), and in our experiments, 10 μM camptothecin killed more than 40% of the treated neurons within 24 h (Fig. 8D). However, Ku-55933 treatment significantly enhanced cell survival levels, demonstrating that camptothecin-induced death was dependent on ATM activity and camptothecin-dependent activation of the DNA damage response pathway triggered apoptosis (Fig. 8D).

Activation of the ATR pathway was seen by immunoblot analysis using phospho-ATR antibodies that recognize the activated form of the protein, in both homocysteine and camptothecin-treated cells (Fig. 9A, lane 1; 9C, lane 1). ATM and ATR activation causes the phosphorylation and activation of Chk1 and Chk2 (Zhou and Elledge, 2000; Brown and Baltimore, 2003; Roos and Kaina, 2006; Pabla *et al.,* 2008). Chk1 and Chk2 in turn can inhibit cell cycle progression, induce the expression of DNA repair enzymes, or ultimately mediate apoptosis if the damage is irreparable (Takai *et al.,* 2000; Maude and Enders, 2005; Vitale *et al.,* 2008). Immunoblot analysis with phospho-Chk1 or phospho-Chk2 antibodies was performed with lysates from neurons treated with homocysteine. Both Chk1 and Chk2 were phosphorylated in response to homocysteine treatment (Fig. 9A, lanes 2 and 3, and 9B). Interestingly, we found that the two checkpoint kinases have different kinetic responses

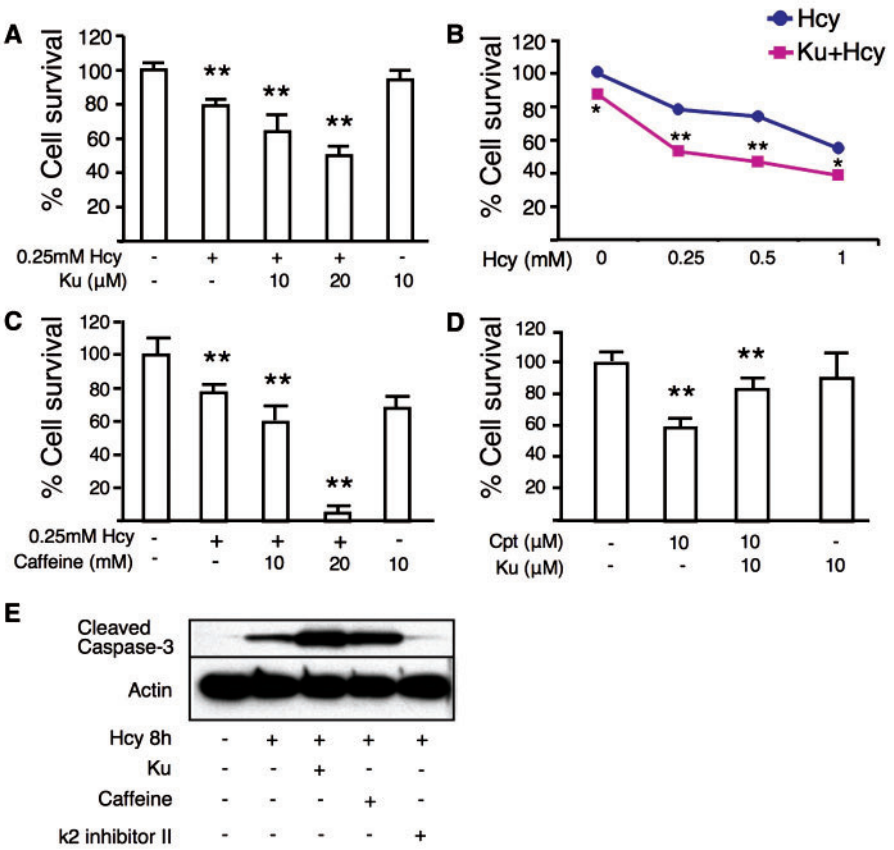

Figure 8 ATM/ATR inhibitors enhance apoptotic death in homocysteine-treated cortical neurons. Cultures were pre-treated with (**A**) 0, 10 or 20 μM Ku-55933 for 1 h before addition of 0.25 mM homocysteine (Hcy); or (**B**) with 10 μM Ku-55933 for 1 h before addition of 0, 0.25, 0.5 or 1 mM homocysteine; or (**C**) with 0, 10 or 20 mM caffeine for 1 h before addition of 0.25 mM homocysteine. Cell survival ratio was evaluated using CellTiter-Glo assay after 40 h. (**D**) Cultures pretreated with 10 μM Ku-55933 for 1 h before addition of 0 or 10 μM camptothecin (Cpt). Cell survival was evaluated after 24 h. $*P<0.01$, $**P<0.001$, *P*-values resulted from Student's *t*-test. Each data point is the mean ± SD ($n=6$). (**E**) Neurons were pretreated with K2 inhibitor II, Ku-55933 or caffeine for 1 h before homocysteine addition. Immunoblot analysis of lysates using cleaved caspase-3 antibodies was performed.

during the time course of homocysteine treatment. Detection of phospho-Chk2 increased rapidly between 1 and 4 h of exposure (Fig. 9A, lane 3), but decreased by 8 h. Phospho-Chk1 was not increased until 8 h and continued to increase up to 24 h of treatment (Fig. 9A, lane 2).

Treatment with both homocysteine and caffeine, which blocks ATR activation, reduced the detection of phospho-ATR (Fig. 9C, lane 1), while Ku-55933 treatment, which primarily inactivates ATM, did not affect ATR activation. Treatment of neurons with homocysteine and Ku-55933, however, significantly reduced but did not eliminate, Chk1 phosphorylation (Fig. 9B), verifying that Ku-55933 prevented the activation of the homocysteine-dependent DNA damage response pathway activation. Phospho-ATR, phospho-Chk1 and phospho-Chk2 were also detected following camptothecin treatment (Fig. 9A, lanes 1–3). When neurons were treated with both Ku-55933 and camptothecin, phospho-ATR and phospho-Chk1 detection was reduced, but phospho-Chk2 activity was blocked completely (Fig. 9A, lanes 1–3).

The tumour suppressor p53 has been shown to play an essential role in the apoptosis induction seen in response to DNA damage in camptothecin treated cortical neurons (Martin *et al.*, 2008). In the absence of DNA damage, p53 is poorly phosphorylated and rapidly degraded. In the presence of DNA damage, Chk1 and Chk2, among other proteins, can phosphorylate and stabilize p53. To determine whether p53 became phosphorylated and was stabilized in response to homocysteine-induced DNA damage, we used phospho-p53 antibodies in immunoblot analysis from lysates of treated neurons. Phosphorylation of p53 was not detected in untreated, differentiated neurons, but became weakly visible between 8 and 24 h of homocysteine treatment (Fig. 9A, lane 5). However, 8 h of campothecin treatment permitted the detection of strong p53 phorphorylation, which was lost in the presence of Ku-55933 treatment (Fig. 9A, lane 5). Thus, while DNA damage is seen in response to homocysteine treatment (Figs 7 and 9C, lane 5), apoptosis induction by homocysteine seems p53-independent, and is distinct from the damage induced by campothecin.

Homocysteine treatment appeared to activate the DNA damage response pathway as seen by phosphorylation of ATR, Chk1 and Chk2, and Ku-55933 or caffeine treatment appeared to reduce this activation. Blocking the DNA damage response pathway by either Ku-55933 or caffeine, however, was unable to rescue neurons from homocysteine-induced death (Fig. 8) and in fact

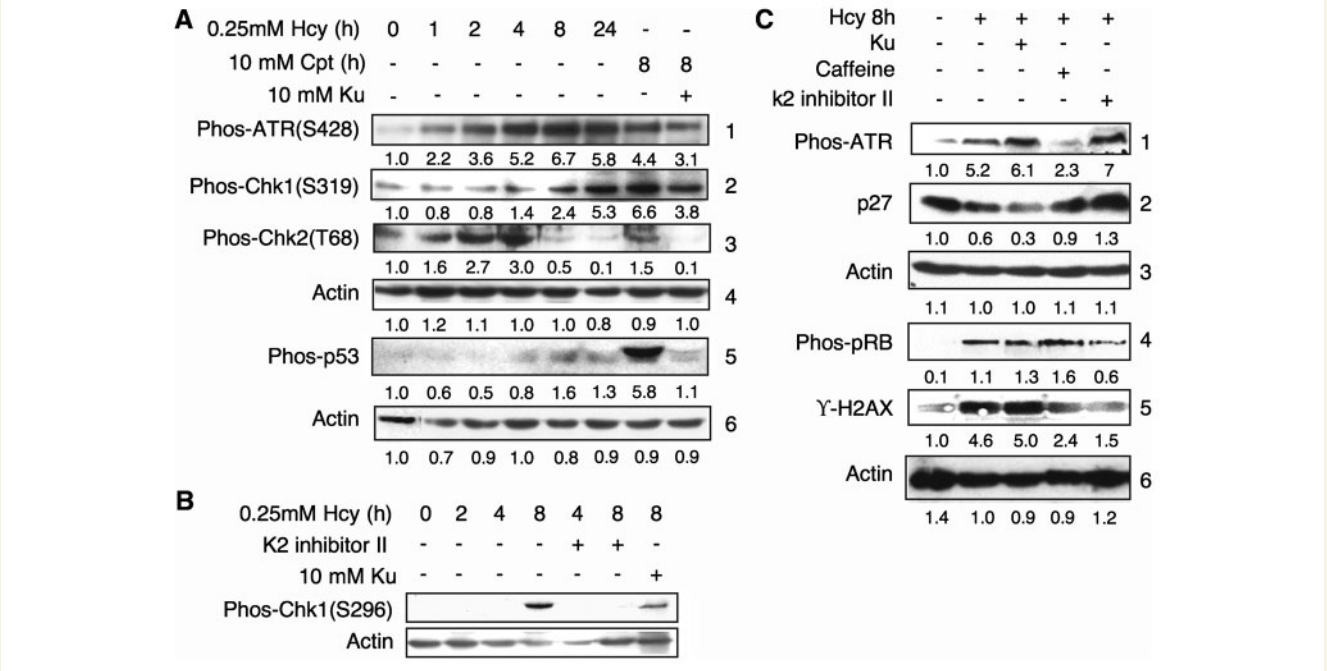

Figure 9 Homocysteine activates the ATR-Chk1/Chk2 pathway. Neurons were pretreated with Ku-55933, caffeine or K2 inhibitor II for 1 h, before homocysteine (Hcy) addition for the indicated time. Cells were lysed and used in immunoblot analysis with (**A**) phospho-ATR (S428) (lane 1), phospho-Chk1 (S319) (lane 2), phospho-Chk2 (T68) (lane 3) and phospho-p53 antibodies (lane 5); (**B**) phospho-Chk1 (S296) antibodies; or (**C**) phospho-ATR (lane 1), p27 (lane 2), phospho-Rb (lane 4) and γ-H2AX (lane 5) antibodies. Actin was used as a loading control. Densitometric quantitation of the immunoblots was performed using Image J software.

exacerbated neuronal apoptosis. We wanted to determine whether blocking the DNA damage response pathway had any affect on cell cycle reactivation. Lysates from neurons treated with homocysteine and different inhibitors (Ku-55933, caffeine or K2 inhibitor II) were examined by immunoblot analysis to examine the levels of the G1 cell cycle proteins. Ku-55933 or caffeine pre-treatment did not block homocysteine-induced G1 cell cycle progression or activation: p27 levels were reduced (Fig. 9C, lane 2) and Rb became phosphorylated (Fig. 9C, lane 4), suggesting that homocysteine treatment initiated cell cycle re-entry independently of the activation status of the DNA damage response pathway. This was in contrast to what was seen when neurons were treated with homocysteine and K2 inhibitor II. As shown in Figs 4B and C and 5A, and again in Fig. 9C, pre-treatment with K2 inhibitor II prevented homocysteine-induced cell cycle reactivation and blocked neuronal cell death. The homocysteine-dependent reduction in p27 levels was not detected (Fig. 9C, lane 2), and phospho-Rb was only weakly detected compared to the levels seen with homocysteine alone, homocysteine and Ku-55933 or homocysteine and caffeine (Fig. 9C, lane 4). Without cell cycle re-entry (no homocysteine or homocysteine and K2 inhibitor II treatment), H2AX phosphorylation was reduced, compared to levels seen in homocysteine alone or with homocysteine and Ku-55933 (Fig. 9C, lane 5). H2AX phosphorylation was detected even in the presence of Ku-55933 treatment (Fig. 9C, lane 5), as it can be phosphorylated by other replication stress-induced kinases, such as ATR or DNA-dependent protein kinase (Park *et al.,* 2003; Chanoux *et al.,* 2009). The homocysteine and K2 inhibitor II treated neurons only partially activated the DNA damage response pathway. Phospho-ATR was detected by immunoblot analysis (Fig. 9C, lane 1), but Chk1 phosphorylation was prevented by the presence of the K2 inhibitor II (Fig. 9B). While ATR was activated in response to homocysteine treatment, in the absence of cdk2 activity and cell cycle progression, it appeared unable to propagate the complete DNA damage response signal.

Discussion

The reappearance of cell cycle markers is one of the earliest abnormalities seen in affected neurons in patients with Alzheimer's disease, but the significance of this remains unclear (Webber *et al.,* 2005; Herrup and Yang, 2007). Investigation into the pathways that stimulate cell cycle re-entry is both necessary to elucidate this process as well to provide potential therapeutic targets. We demonstrated that homocysteine treatment of differentiated, quiescent cortical neurons in culture caused reactivation of the G1 cell cycle proteins, permitting transit into S phase. Homocysteine treatment caused cyclin D1, cdk4 and cdk2 nuclear translocation and down-regulation of the cdk inhibitor p27Kip1. Reactivation of the cell cycle machinery was required for homocysteine-induced apoptosis as blocking the G1 cell cycle proteins, by a variety of methods, prevented neuronal cell death. Cell cycle re-entry permitted entry into S phase and subsequent DNA synthesis, and it appeared that S phase entry was required to trigger apoptosis. We observed a 95% co-localization of DNA synthesis and apoptosis markers in homocysteine-treated neurons,

suggesting that cells that started DNA replication ultimately died. However, blocking cell cycle progression post G1, using DNA synthesis inhibitors, was unable to prevent apoptosis, suggesting that death was not preventable after the G1–S phase checkpoint.

Interestingly, the G0–G1–S phase transition seen in cultured neurons remarkably resembles the mitogen-dependent G0–G1–S phase transition seen in epithelial or lymphoid cells (Sherr and Roberts, 1999; Becker and Bonni, 2004; Bockstaele *et al.,* 2006). In both scenarios, cyclin D1 moves to the nucleus, where it partners with cdk4. Cdk4 and cdk2 phosphorylate Rb, which permits entry into S phase and DNA replication initiation. The outcome, however, is different and suggests that differentiated neurons may no longer be competent to complete S phase or the entire cell cycle. Apoptosis is required during the development of the nervous system (Becker and Bonni, 2004, 2005). However, DNA synthesis and activation of cell cycle proteins is not detected in apoptosis in the developing brain, suggesting that DNA synthesis in 'post-mitotic' neurons may be a death signal.

How homocysteine reactivates the cell cycle is not clear, but direct effects on cyclin D1 and p27 seem likely. These are critical sensors in epithelial and lymphoid cells, sensitive to a variety of soluble mitogenic and antimitogenic factors, as well as cell–cell and cell–extracellular matrix interactions (Nickeleit *et al.,* 2007; Malumbres and Barbacid, 2009). Proteins, such as glycogen synthase kinase 3-β (Pontano and Diehl, 2009) or S-phase kinase-associated protein 2 (Frescas and Pagano, 2008), which regulate mitogen-dependent cyclin D1 nuclear translocation and p27 degradation, respectively, in these cell types, might be involved in homocysteine-dependent cell cycle re-entry as well. We were able to block homocysteine-dependent apoptosis by inhibition of G1 cell cycle progression at multiple different steps, stressing the importance of the entire G1 cell cycle phase rather than the significance of any one protein, and highlighting the plethora of potential therapeutic targets this pathway presents. This is consistent with the proposed linearity and temporal order of the 'Rb pathway' during the G0–G1 phase transition in epithelial or lymphoid cells, where cyclin D–cdk4 may be required to activate cdk2, which in turn may be required to target p27 for degradation; and the combined contribution of both cdk4 and cdk2 may be needed for full Rb phosphorylation and S phase entry (Blain, 2008; Malumbres and Barbacid, 2009).

In our model we tested a physiological Alzheimer's disease risk factor, homocysteine, which is produced as a natural by-product of methionine metabolism. Increased levels of total plasma homocysteine can be caused by genetic defects, nutritional deficiencies in folate, vitamin B12, vitamin B6 or other factors (Welch and Loscalzo, 1998; Gueant *et al.,* 2005). Elevated plasma homocysteine concentrations were found in patients with chronic renal failure (Wilcken and Gupta, 1979; Chauveau *et al.,* 1993), hypothyroidism (McCully, 1996) and pernicious anaemia (Savage *et al.,* 1994). Hyperhomocysteinaemia was shown to be a strong, independent risk factor for dementia and Alzheimer's disease (Seshadri *et al.,* 2002; Mizrahi *et al.,* 2004; Agnati *et al.,* 2005; Ravaglia *et al.,* 2005; Blasko *et al.,* 2008), Parkinson's disease (Mattson and Shea, 2003) and stroke (Hankey and Eikelboom, 2001). Elevations in plasma homocysteine levels precede the development of dementia and there is a continuous, inverse linear relation between plasma homocysteine concentrations and cognitive performance in aged adults (McCaddon *et al.,* 1998; Irizarry *et al.,* 2005; Kado *et al.,* 2005). Hyperhomocysteinaemia also appears to exacerbate the effects of other factors implicated in Alzheimer's disease pathology, such as increasing tau phosphorylation and beta-amyloid toxicity (Pacheco-Quinto *et al.,* 2006; Luo *et al.,* 2007). Neuronal apoptosis has been detected in the hippocampal and cortical neurons of folate deficient mouse models (Kruman *et al.,* 2000, 2005). While others have studied the effects of genotoxic or DNA damaging agents as inducers of neuronal apoptosis, we chose homocysteine not only for its physiological significance but because its ability to inflict DNA damage was more subtle. Extended hyperhomocysteinaemia in patients may cause a similar cell cycle re-entry in affected neurons, which might eventually contribute to neuronal cell loss.

DNA damage occurs in response to toxic chemicals, as a byproduct of normal metabolism through the generation of reactive oxygen species or free radicals, or through errors in DNA replication, such as DNA replication fork stalling due to low nucleotide pools or blocking DNA lesions. Our results demonstrated that homocysteine did cause DNA damage as seen by increases in Comet positive neurons. However, the appearance of γ-H2AX suggests that homocysteine-induced DNA damage may be due to replication stress rather than more traditional DNA breaks, such as caused by DNA damaging agents like camptothecin. Homocysteine activates the DNA damage response, as seen by phosphorylation of ATR, Chk1 and Chk2, but the DNA damage response induced by homocysteine appears different than the DNA damage response induced by camptothecin. The homocysteine-induced DNA damage response appears to be p53-independent and inhibition of ATM/ATR activity does not block apoptosis, but rather exacerbates it. This is in stark contrast to the actions of camptothecin, which appears to induce p53, and be ATM/ATR dependent: apoptosis is blocked when these proteins are inhibited. The 95% colocalization of S phase markers and apoptotic markers suggests that homocysteine-induced apoptosis is due to S phase entry, and subsequent DNA replication stalling might be the cause of DNA damage, activating the DNA damage response. The activation of the DNA damage response pathway was not responsible for homocysteine-dependent neuronal cell death, as inhibition of this pathway accelerated the induction of apoptosis, suggesting that it may have a more neuroprotective function. Support for this idea comes from recent studies that have shown that the ATR-Chk1 pathway can protect HCT116 cells from caspase-3-dependent apoptosis, suggesting that the pathways that protect from replication stress are different than those induced by more traditional DNA damaging agents (Myers *et al.,* 2009). Others have demonstrated that agents like etoposide or methotrexate (Kruman *et al.,* 2004), camptothecin (Martin *et al.,* 2008; Tian *et al.,* 2009), ultraviolet irradiation (Park *et al.,* 1998), γ-irradiation (Enokido *et al.,* 1996) and arabinoside (Tomkins *et al.,* 1994) directly and irreparably damage DNA and induce apoptosis. Our data suggest that homocysteine causes apoptosis by a different mechanism, directly causing the G0–S phase transition, with the DNA damage response pathway only activated to block the S phase-dependent apoptotic response.

While others have suggested that DNA damage itself is the causative agent of cell cycle reactivation and DNA synthesis (Kruman *et al.,* 2004; Tian *et al.,* 2009), in our system, we found that blocking the DNA damage response pathway with Ku or caffeine treatment, did not block cell cycle re-entry, as seen by p27 down-regulation and Rb phosphorylation. Neurons still entered S phase, but in the absence of the protective effect of the DNA damage response, apoptosis was increased. Conversely, blocking cell cycle re-entry with K2 inhibitor II also decreased γ-H2AX detection, presumably due to decreased DNA synthesis, but did not block ATR activation. Clearly, the two pathways are interconnected: DNA synthesis increases DNA damage that activates the DNA damage response pathway that feedbacks and attempts to halt and/or repair synthesis-induced damage, but at least to some extent they function independently. We would suggest that the nature of the initiating agent, homocysteine versus camptothecin, and the type of ensuing DNA damage (replication stress versus double-strand breaks) might explain the difference between our results and those of others.

The parallels between mitogen-induced G0 exit in epithelial and lymphoid cells and differentiated neurons should not be overlooked. We were able to block homocysteine-induced death only by blocking G1 phase progression. Once the neuron had reached S phase and began to replicate DNA, apoptosis could not be prevented and activation of the DNA damage response may only be prolonging an inevitable death. The appearance of cell cycle markers in neurodegenerative disease *in vivo* might represent a state that is already retractable to intervention, and the real challenge may be to prevent the initial G1–S phase progression. Cell cycle proteins have been therapeutic targets in cancer drug development for decades and it will be interesting to determine whether these types of inhibitors might be useful in the treatment of neurodegenerative disease as well.

Acknowledgements

Gleevec™ (STI571 mesylate salt) was a kind gift from Novartis Pharmaceuticals. We thank Dr Ting-Chung Suen and Dr Sarah Nataraj for helpful discussion, and Dr William Oxberry for help with confocal microscopy techniques.

Funding

American Cancer Society (to S.W.B.); and a National Institute of Aging Leadership Award in Alzheimer's Disease Research (grant number 5 K07 AG00959 to Dr Suzanne Mirra).

References

Adams RL, Lindsay JG. Hydroxyurea reversal of inhibition and use as a cell-synchronizing agent. J Biol Chem 1967; 242: 1314–7.

Agnati LF, Genedani S, Rasio G, Galantucci M, Saltini S, Filaferro M, et al. Studies on homocysteine plasma levels in Alzheimer's patients. Relevance for neurodegeneration. J Neural Transm 2005; 112: 163–9.

Akashiba H, Matsuki N, Nishiyama N. Calpain activation is required for glutamate-induced p27 down-regulation in cultured cortical neurons. J Neurochem 2006a; 99: 733–44.

Akashiba H, Matsuki N, Nishiyama N. p27 small interfering RNA induces cell death through elevating cell cycle activity in cultured cortical neurons: a proof-of-concept study. Cell Mol Life Sci 2006b; 63: 2397–404.

Alvarez AR, Sandoval PC, Leal NR, Castro PU, Kosik KS. Activation of the neuronal c-Abl tyrosine kinase by amyloid-beta-peptide and reactive oxygen species. Neurobiol Dis 2004; 17: 326–36.

Andreotti PE, Cree IA, Kurbacher CM, Hartmann DM, Linder D, Harel G, et al. Chemosensitivity testing of human tumors using a microplate adenosine triphosphate luminescence assay: clinical correlation for cisplatin resistance of ovarian carcinoma. Cancer Res 1995; 55: 5276–82.

Angelastro JM, Moon NY, Liu DX, Yang AS, Greene LA, Franke TF. Characterization of a novel isoform of caspase-9 that inhibits apoptosis. J Biol Chem 2001; 276: 12190–200.

Angelis KJ, Dusinska M, Collins AR. Single cell gel electrophoresis: detection of DNA damage at different levels of sensitivity. Electrophoresis 1999; 20: 2133–8.

Avramis IA, Laug WE, Sausville EA, Avramis VI. Determination of drug synergism between the tyrosine kinase inhibitors NSC 680410 (adaphostin) and/or STI571 (imatinib mesylate, Gleevec) with cytotoxic drugs against human leukemia cell lines. Cancer Chemother Pharmacol 2003; 52: 307–18.

Bartek J, Lukas J. DNA damage checkpoints: from initiation to recovery or adaptation. Curr Opin Cell Biol 2007; 19: 238–45.

Becker EB, Bonni A. Cell cycle regulation of neuronal apoptosis in development and disease. Prog Neurobiol 2004; 72: 1–25.

Becker EB, Bonni A. Beyond proliferation – cell cycle control of neuronal survival and differentiation in the developing mammalian brain. Semin Cell Dev Biol 2005; 16: 439–48.

Besson A, Dowdy SF, Roberts JM. CDK inhibitors: cell cycle regulators and beyond. Dev Cell 2008; 14: 159–69.

Blain SW. Switching cyclin D-Cdk4 kinase activity on and off. Cell Cycle 2008; 7: 892–8.

Blasko I, Jellinger K, Kemmler G, Krampla W, Jungwirth S, Wichart I, et al. Conversion from cognitive health to mild cognitive impairment and Alzheimer's disease: prediction by plasma amyloid beta 42, medial temporal lobe atrophy and homocysteine. Neurobiol Aging 2008; 29: 1–11.

Bockstaele L, Coulonval K, Kooken H, Paternot S, Roger PP. Regulation of CDK4. Cell Div 2006; 1: 25.

Bonda DJ, Evans TA, Santocanale C, Llosa JC, Vina J, Bajic VP, et al. Evidence for the progression through S-phase in the ectopic cell cycle re-entry of neurons in Alzheimer disease. Aging (Albany NY) 2009; 1: 382–8.

Brown EJ, Baltimore D. Essential and dispensable roles of ATR in cell cycle arrest and genome maintenance. Genes Dev 2003; 17: 615–28.

Busciglio J, Yankner BA. Apoptosis and increased generation of reactive oxygen species in Down's syndrome neurons in vitro. Nature 1995; 378: 776–9.

Cancino GI, Toledo EM, Leal NR, Hernandez DE, Yevenes LF, Inestrosa NC, et al. STI571 prevents apoptosis, tau phosphorylation and behavioural impairments induced by Alzheimer's beta-amyloid deposits. Brain 2008; 131: 2425–42.

Carey RG, Li B, DiCicco-Bloom E. Pituitary adenylate cyclase activating polypeptide anti-mitogenic signaling in cerebral cortical progenitors is regulated by p57Kip2-dependent CDK2 activity. J Neurosci 2002; 22: 1583–91.

Chanoux R, Yin B, Urtishak K, Asare A, Bassing C, Brown E. ATR and H2AX cooperate in maintaining genome stability under replication stress. J Biol Chem 2009; 284: 5994–6003.

Chauveau P, Chadefaux B, Coude M, Aupetit J, Hannedouche T, Kamoun P, et al. Hyperhomocysteinemia, a risk factor for atherosclerosis in chronic uremic patients. Kidney Int Suppl 1993; 41: S72–7.

Chen Y, McPhie DL, Hirschberg J, Neve RL. The amyloid precursor protein-binding protein APP-BP1 drives the cell cycle through the S-M

checkpoint and causes apoptosis in neurons. J Biol Chem 2000; 275: 8929–35.
Clarke R. Homocysteine and cardiovascular disease. Overview. J Cardiovasc Risk 1998; 5: 213–5.
Cooper-Kuhn CM, Kuhn HG. Is it all DNA repair? Methodological considerations for detecting neurogenesis in the adult brain. Brain Res Dev Brain Res 2002; 134: 13–21.
Copani A, Condorelli F, Caruso A, Vancheri C, Sala A, Giuffrida Stella AM, et al. Mitotic signaling by beta-amyloid causes neuronal death. Faseb J 1999; 13: 2225–34.
Crouch SP, Kozlowski R, Slater KJ, Fletcher J. The use of ATP bioluminescence as a measure of cell proliferation and cytotoxicity. J Immunol Methods 1993; 160: 81–8.
Davis ST, Benson BG, Bramson HN, Chapman DE, Dickerson SH, Dold KM, et al. Prevention of chemotherapy-induced alopecia in rats by CDK inhibitors. Science 2001; 291: 134–7.
Enokido Y, Araki T, Tanaka K, Aizawa S, Hatanaka H. Involvement of p53 in DNA strand break-induced apoptosis in postmitotic CNS neurons. Eur J Neurosci 1996; 8: 1812–21.
Frescas D, Pagano M. Deregulated proteolysis by the F-box proteins SKP2 and beta-TrCP: tipping the scales of cancer. Nat Rev Cancer 2008; 8: 438–49.
Giovanni A, Wirtz-Brugger F, Keramaris E, Slack R, Park DS. Involvement of cell cycle elements, cyclin-dependent kinases, pRb, and E2F x DP, in B-amyloid-induced neuronal death. J Biol Chem 1999; 274: 19011–6.
Gladden AB, Diehl JA. Location, location, location: the role of cyclin D1 nuclear localization in cancer. J Cell Biochem 2005; 96: 906–13.
Gonchoroff NJ, Katzmann JA, Currie RM, Evans EL, Houck DW, Kline BC, et al. S-phase detection with an antibody to bromodeoxyuridine. Role of DNase pretreatment. J Immunol Methods 1986; 93: 97–101.
Gueant JL, Anello G, Bosco P, Gueant-Rodriguez RM, Romano A, Barone C, et al. Homocysteine and related genetic polymorphisms in Down's syndrome IQ. J Neurol Neurosurg Psychiatry 2005; 76: 706–9.
Hagerkvist R, Sandler S, Mokhtari D, Welsh N. Amelioration of diabetes by imatinib mesylate (Gleevec): role of beta-cell NF-kappaB activation and anti-apoptotic preconditioning. Faseb J 2007; 21: 618–28.
Hankey GJ, Eikelboom JW. Homocysteine and stroke. Curr Opin Neurol 2001; 14: 95–102.
Herrup K, Yang Y. Cell cycle regulation in the postmitotic neuron: oxymoron or new biology? Nat Rev Neurosci 2007; 8: 368–78.
Hickson I, Zhao Y, Richardson CJ, Green SJ, Martin NM, Orr AI, et al. Identification and characterization of a novel and specific inhibitor of the ataxia-telangiectasia mutated kinase ATM. Cancer Res 2004; 64: 9152–9.
Irizarry MC, Gurol ME, Raju S, Diaz-Arrastia R, Locascio JJ, Tennis M, et al. Association of homocysteine with plasma amyloid beta protein in aging and neurodegenerative disease. Neurology 2005; 65: 1402–8.
James MK, Ray A, Leznova D, Blain SW. Differential modification of p27Kip1 controls its cyclin D-cdk4 inhibitory activity. Mol Cell Biol 2008; 28: 498–510.
Jellinger KA. Challenges in neuronal apoptosis. Curr Alzheimer Res 2006; 3: 377–91.
Jimenez del Rio M, Velez-Pardo C. Apoptosis in neurodegenerative diseases: facts and controversies. Rev Neurol 2001; 32: 851–60.
Kado DM, Karlamangla AS, Huang MH, Troen A, Rowe JW, Selhub J, et al. Homocysteine versus the vitamins folate, B6, and B12 as predictors of cognitive function and decline in older high-functioning adults: MacArthur Studies of Successful Aging. Am J Med 2005; 118: 161–7.
Knudsen ES, Wang JY. Dual mechanisms for the inhibition of E2F binding to RB by cyclin-dependent kinase-mediated RB phosphorylation. Mol Cell Biol 1997; 17: 5771–83.
Kowalzick L, Gauri KK, Spadari S, Pedrali-Noy G, Kuhne J, Koch G. Differential incorporation of thymidylate analogues into DNA by DNA polymerase alpha and by DNA polymerases specified by two herpes simplex viruses. J Gen Virol 1982; 62 (Pt 1): 29–38.
Kruman II, Culmsee C, Chan SL, Kruman Y, Guo Z, Penix L, et al. Homocysteine elicits a DNA damage response in neurons that promotes apoptosis and hypersensitivity to excitotoxicity. J Neurosci 2000; 20: 6920–6.
Kruman II, Mouton PR, Emokpae R Jr, Cutler RG, Mattson MP. Folate deficiency inhibits proliferation of adult hippocampal progenitors. Neuroreport 2005; 16: 1055–9.
Kruman II, Wersto RP, Cardozo-Pelaez F, Smilenov L, Chan SL, Chrest FJ, et al. Cell cycle activation linked to neuronal cell death initiated by DNA damage. Neuron 2004; 41: 549–61.
Kubo A, Nakagawa K, Varma RK, Conrad NK, Cheng JQ, Lee WC, et al. The p16 status of tumor cell lines identifies small molecule inhibitors specific for cyclin-dependent kinase 4. Clin Cancer Res 1999; 5: 4279–86.
Lemay M, Wood KA. Detection of DNA damage and identification of UV-induced photoproducts using the CometAssay kit. Biotechniques 1999; 27: 846–51.
Liu DX, Greene LA. Neuronal apoptosis at the G1/S cell cycle checkpoint. Cell Tissue Res 2001; 305: 217–28.
Lu YP, Lou YR, Peng QY, Xie JG, Nghiem P, Conney AH. Effect of caffeine on the ATR/Chk1 pathway in the epidermis of UVB-irradiated mice. Cancer Res 2008; 68: 2523–9.
Luo Y, Zhou X, Yang X, Wang J. Homocysteine induces tau hyperphosphorylation in rats. Neuroreport 2007; 18: 2005–8.
Malumbres M, Barbacid M. Cell cycle, CDKs and cancer: a changing paradigm. Nat Rev Cancer 2009; 9: 153–66.
Martin LJ, Liu Z, Pipino J, Chestnut B, Landek MA. Molecular regulation of DNA damage-induced apoptosis in neurons of cerebral cortex. Cereb Cortex 2008; 19: 1278–93.
Martinez G, Di Giacomo C, Carnazza ML, Sorrenti V, Castana R, Barcellona ML, et al. MAP2, synaptophysin immunostaining in rat brain and behavioral modifications after cerebral postischemic reperfusion. Dev Neurosci 1997; 19: 457–64.
Mattson MP, Shea TB. Folate and homocysteine metabolism in neural plasticity and neurodegenerative disorders. Trends Neurosci 2003; 26: 137–46.
Maude SL, Enders GH. Cdk inhibition in human cells compromises chk1 function and activates a DNA damage response. Cancer Res 2005; 65: 780–6.
McCaddon A, Davies G, Hudson P, Tandy S, Cattell H. Total serum homocysteine in senile dementia of Alzheimer type. Int J Geriatr Psychiatry 1998; 13: 235–9.
McCully KS. Homocysteine and vascular disease. Nat Med 1996; 2: 386–9.
McShea A, Harris PL, Webster KR, Wahl AF, Smith MA. Abnormal expression of the cell cycle regulators P16 and CDK4 in Alzheimer's disease. Am J Pathol 1997; 150: 1933–9.
Mehra RD, Hendrickson AE. A comparison of the development of neuropeptide and MAP2 immunocytochemical labeling in the macaque visual cortex during pre- and postnatal development. J Neurobiol 1993; 24: 101–24.
Mizrahi EH, Bowirrat A, Jacobsen DW, Korczyn AD, Traore F, Petot GJ, et al. Plasma homocysteine, vitamin B12 and folate in Alzheimer's patients and healthy Arabs in Israel. J Neurol Sci 2004; 227: 109–13.
Morris EJ, Geller HM. Induction of neuronal apoptosis by camptothecin, an inhibitor of DNA topoisomerase-I: evidence for cell cycle-independent toxicity. J Cell Biol 1996; 134: 757–70.
Myers K, Gagou ME, Zuazua-Villar P, Rodriguez R, Meuth M. ATR and Chk1 suppress a caspase-3-dependent apoptotic response following DNA replication stress. PLoS Genet 2009; 5: e1000324.
Nagy Z, Esiri MM, Cato AM, Smith AD. Cell cycle markers in the hippocampus in Alzheimer's disease. Acta Neuropathol 1997; 94: 6–15.
Nagy Z, Esiri MM, Smith AD. The cell division cycle and the pathophysiology of Alzheimer's disease. Neuroscience 1998; 87: 731–9.

Nickeleit I, Zender S, Kossatz U, Malek NP. p27kip1: a target for tumor therapies? Cell Div 2007; 2: 13.

Offen D, Elkon H, Melamed E. Apoptosis as a general cell death pathway in neurodegenerative diseases. J Neural Transm Suppl 2000; 58: 153–66.

Ogawa O, Zhu X, Lee HG, Raina A, Obrenovich ME, Bowser R, et al. Ectopic localization of phosphorylated histone H3 in Alzheimer's disease: a mitotic catastrophe? Acta Neuropathol 2003; 105: 524–8.

Oguro M, Suzuki-Hori C, Nagano H, Mano Y, Ikegami S. The mode of inhibitory action by aphidicolin on eukaryotic DNA polymerase alpha. Eur J Biochem 1979; 97: 603–7.

Pabla N, Huang S, Mi Q, Daniel R, Dong Z. ATR-Chk2 signaling in p53 activation and DNA damage response during cisplatin-induced apoptosis. J Biol Chem 2008; 283: 6572–83.

Pacheco-Quinto J, Rodriguez de Turco EB, DeRosa S, Howard A, Cruz-Sanchez F, Sambamurti K, et al. Hyperhomocysteinemic Alzheimer's mouse model of amyloidosis shows increased brain amyloid beta peptide levels. Neurobiol Dis 2006; 22: 651–6.

Pandita TK. ATM function and telomere stability. Oncogene 2002; 21: 611–8.

Park DS, Farinelli SE, Greene LA. Inhibitors of cyclin-dependent kinases promote survival of post-mitotic neuronally differentiated PC12 cells and sympathetic neurons. J Biol Chem 1996; 271: 8161–9.

Park DS, Morris EJ, Greene LA, Geller HM. G1/S cell cycle blockers and inhibitors of cyclin-dependent kinases suppress camptothecin-induced neuronal apoptosis. J Neurosci 1997; 17: 1256–70.

Park DS, Morris EJ, Padmanabhan J, Shelanski ML, Geller HM, Greene LA. Cyclin-dependent kinases participate in death of neurons evoked by DNA-damaging agents. J Cell Biol 1998; 143: 457–67.

Park EJ, Chan DW, Park JH, Oettinger MA, Kwon J. DNA-PK is activated by nucleosomes and phosphorylates H2AX within the nucleosomes in an acetylation-dependent manner. Nucleic Acids Res 2003; 31: 6819–27.

Pontano LL, Diehl JA. DNA damage-dependent cyclin D1 proteolysis: GSK3beta holds the smoking gun. Cell Cycle 2009; 8: 824–7.

Qiu J, Takagi Y, Harada J, Topalkara K, Wang Y, Sims JR, et al. p27Kip1 constrains proliferation of neural progenitor cells in adult brain under homeostatic and ischemic conditions. Stem Cells 2009; 27: 920–7.

Raina AK, Hochman A, Zhu X, Rottkamp CA, Nunomura A, Siedlak SL, et al. Abortive apoptosis in Alzheimer's disease. Acta Neuropathol 2001; 101: 305–10.

Raina AK, Zhu X, Rottkamp CA, Monteiro M, Takeda A, Smith MA. Cyclin' toward dementia: cell cycle abnormalities and abortive oncogenesis in Alzheimer disease. J Neurosci Res 2000; 61: 128–33.

Raina AK, Zhu X, Smith MA. Alzheimer's disease and the cell cycle. Acta Neurobiol Exp (Wars) 2004; 64: 107–12.

Ravaglia G, Forti P, Maioli F, Martelli M, Servadei L, Brunetti N, et al. Homocysteine and folate as risk factors for dementia and Alzheimer disease. Am J Clin Nutr 2005; 82: 636–43.

Rich T, Allen RL, Wyllie AH. Defying death after DNA damage. Nature 2000; 407: 777–83.

Roos WP, Kaina B. DNA damage-induced cell death by apoptosis. Trends Mol Med 2006; 12: 440–50.

Rotman G, Shiloh Y. ATM: a mediator of multiple responses to genotoxic stress. Oncogene 1999; 18: 6135–44.

Sarkaria JN, Busby EC, Tibbetts RS, Roos P, Taya Y, Karnitz LM, et al. Inhibition of ATM and ATR kinase activities by the radiosensitizing agent, caffeine. Cancer Res 1999; 59: 4375–82.

Savage DG, Lindenbaum J, Stabler SP, Allen RH. Sensitivity of serum methylmalonic acid and total homocysteine determinations for diagnosing cobalamin and folate deficiencies. Am J Med 1994; 96: 239–46.

Seshadri S, Beiser A, Selhub J, Jacques PF, Rosenberg IH, D'Agostino RB, et al. Plasma homocysteine as a risk factor for dementia and Alzheimer's disease. N Engl J Med 2002; 346: 476–83.

Sethi CS, Lewis GP, Fisher SK, Leitner WP, Mann DL, Luthert PJ, et al. Glial remodeling and neural plasticity in human retinal detachment with proliferative vitreoretinopathy. Invest Ophthalmol Vis Sci 2005; 46: 329–42.

Shan J, Munro TP, Barbarese E, Carson JH, Smith R. A molecular mechanism for mRNA trafficking in neuronal dendrites. J Neurosci 2003; 23: 8859–66.

Sherr CJ, McCormick F. The RB and p53 pathways in cancer. Cancer Cell 2002; 2: 103–12.

Sherr CJ, Roberts JM. Inhibitors of mammalian G1 cyclin-dependent kinases. Genes Dev 1995; 9: 1149–63.

Sherr CJ, Roberts JM. CDK inhibitors: positive and negative regulators of G1-phase progression. Genes Dev 1999; 13: 1501–12.

Shiloh Y. ATM and related protein kinases: safeguarding genome integrity. Nat Rev Cancer 2003; 3: 155–68.

Shuai XM, Han GX, Wang GB, Chen JH. Cyclin D1 antisense oligodexoyneucleotides inhibits growth and enhances chemosensitivity in gastric carcinoma cells. World J Gastroenterol 2006; 12: 1766–9.

Staker BL, Hjerrild K, Feese MD, Behnke CA, Burgin AB Jr, Stewart L. The mechanism of topoisomerase I poisoning by a camptothecin analog. Proc Natl Acad Sci USA 2002; 99: 15387–92.

Sumrejkanchanakij P, Tamamori-Adachi M, Matsunaga Y, Eto K, Ikeda MA. Role of cyclin D1 cytoplasmic sequestration in the survival of postmitotic neurons. Oncogene 2003; 22: 8723–30.

Takai H, Tominaga K, Motoyama N, Minamishima YA, Nagahama H, Tsukiyama T, et al. Aberrant cell cycle checkpoint function and early embryonic death in Chk1(-/-) mice. Genes Dev 2000; 14: 1439–47.

Tanaka T, Halicka HD, Traganos F, Seiter K, Darzynkiewicz Z. Induction of ATM activation, histone H2AX phosphorylation and apoptosis by etoposide: relation to cell cycle phase. Cell Cycle 2007; 6: 371–6.

Thakur A, Siedlak SL, James SL, Bonda DJ, Rao A, Webber KM, et al. Retinoblastoma protein phosphorylation at multiple sites is associated with neurofibrillary pathology in Alzheimer disease. Int J Clin Exp Pathol 2008; 1: 134–46.

Tian B, Yang Q, Mao Z. Phosphorylation of ATM by Cdk5 mediates DNA damage signalling and regulates neuronal death. Nat Cell Biol 2009; 11: 211–8.

Tice RR, Agurell E, Anderson D, Burlinson B, Hartmann A, Kobayashi H, et al. Single cell gel/comet assay: guidelines for in vitro and in vivo genetic toxicology testing. Environ Mol Mutagen 2000; 35: 206–21.

Tomkins CE, Edwards SN, Tolkovsky AM. Apoptosis is induced in post-mitotic rat sympathetic neurons by arabinosides and topoisomerase II inhibitors in the presence of NGF. J Cell Sci 1994; 107 (Pt 6): 1499–507.

Ueyama C, Akashiba H, Nakayama K, Nakayama KI, Nishiyama N, Matsuki N. Ablation of p27 enhance kainate-induced seizure and hippocampal degeneration. Neuroreport 2007; 18: 1781–5.

Vesely J, Havlicek L, Strnad M, Blow JJ, Donella-Deana A, Pinna L, et al. Inhibition of cyclin-dependent kinases by purine analogues. Eur J Biochem 1994; 224: 771–86.

Vitale I, Senovilla L, Galluzzi L, Criollo A, Vivet S, Castedo M, et al. Chk1 inhibition activates p53 through p38 MAPK in tetraploid cancer cells. Cell Cycle 2008; 7: 1956–61.

Webber KM, Raina AK, Marlatt MW, Zhu X, Prat MI, Morelli L, et al. The cell cycle in Alzheimer disease: a unique target for neuropharmacology. Mech Ageing Dev 2005; 126: 1019–25.

Welch GN, Loscalzo J. Homocysteine and atherothrombosis. N Engl J Med 1998; 338: 1042–50.

Wilcken DE, Gupta VJ. Sulphr containing amino acids in chronic renal failure with particular reference to homocystine and cysteine-homocysteine mixed disulphide. Eur J Clin Invest 1979; 9: 301–7.

Yang Y, Mufson EJ, Herrup K. Neuronal cell death is preceded by cell cycle events at all stages of Alzheimer's disease. J Neurosci 2003; 23: 2557–63.

Ye W, Mairet-Coello G, Pasoreck E, Dicicco-Bloom E. Patterns of p57Kip2 expression in embryonic rat brain suggest roles in progenitor cell cycle exit and neuronal differentiation. Dev Neurobiol 2009; 69: 1–21.

Ye W, Zhang L. Heme deficiency causes apoptosis but does not increase ROS generation in HeLa cells. Biochem Biophys Res Commun 2004; 319: 1065–71.

Zhang Y, Qu D, Morris EJ, O'Hare MJ, Callaghan SM, Slack RS, et al. The Chk1/Cdc25A pathway as activators of the cell cycle in neuronal death induced by camptothecin. J Neurosci 2006; 26: 8819–28.

Zhou BB, Elledge SJ. The DNA damage response: putting checkpoints in perspective. Nature 2000; 408: 433–9.

Zhu X, Raina AK, Perry G, Smith MA. Apoptosis in Alzheimer disease: a mathematical improbability. Curr Alzheimer Res 2006; 3: 393–6.

Zindy F, Cunningham JJ, Sherr CJ, Jogal S, Smeyne RJ, Roussel MF. Postnatal neuronal proliferation in mice lacking Ink4d and Kip1 inhibitors of cyclin-dependent kinases. Proc Natl Acad Sci USA 1999; 96: 13462–7.